TAMPEREEN TEKNILLINEN YLIOPISTO
TAMPERE UNIVERSITY OF TECHNOLOGY

JAAKKO TAMMINEN

HEAT TRANSFER BASED FOULING EXAMINATION IN FLUIDIZED BED BOILERS

Master of Science Thesis

Examiner: University Lecturer Henrik Tolvanen
Examiner and topic approved in the Faculty of Natural Sciences Council meeting on 7th of June 2017

ABSTRACT

JAAKKO TAMMINEN: Heat Transfer Based Fouling Examination in Fluidized Bed Boilers
Tampere University of Technology
Master of Science Thesis, 71 pages
November 2017
Master's Degree Programme in Environmental and Energy Engineering
Major: Energy and Biorefining Engineering
Examiner: University Lecturer Henrik Tolvanen

Keywords: fouling, deposition, fouling rate, thermal resistance, fluidized bed, heat transfer, heat exchanger, soot blowing

Fly ash components in the flue gas can stick onto heat exchanger tubes and cumulate into solid deposits. This fouling phenomenon is a common issue in fluidized bed boilers, where challenging fuels with possibly high and challenging ash content are often fired in. Basic characteristics of the phenomenon are discussed briefly, followed by a short review of research on the methods of modelling and predicting fouling tendency. These methods include fuel-based indices, chemical equilibrium modelling, CFD modelling and evaluations based on weight or heat transfer measurements.

A method to examine fouling through heat transfer calculations was tested in this thesis. Primary aim was to verify applicability of this selected method in real large-scale boilers via performing a retrospective analysis on earlier measurement data. Reference clean state heat transfer coefficients of certain heat exchangers were compared to calculated states by using data from control system log files, and the comparisons were formulated into thermal resistances of the deposit layer. The control system log files contained data from earlier measurement campaigns. Calculated thermal resistances increased along cumulating deposition, until a cleansing soot blowing pulse is actuated. Slopes of these rising thermal resistance curves were extracted, forming estimates of fouling rates per each fouling period. Calculated thermal resistance build-ups matched soot blowing operation times well with only a few exceptions, and so the selected method seemed to express actual fouling decently in general.

Calculated resistances and fouling rates were compared to other operational factors, including main steam power, fuel feed variation and measured flue gas pressure change at studied heat exchangers. Certain findings were made, even though available data was not completely sufficient. While decent correlation with slight steam power changes was not identifiable, studying the flue gas pressure change showed very evident relation with thermal resistances. Fuel mixture appeared to affect the fouling rates, but not consistently with small changes in the fuel feed. Conclusions of fouling differences between superheater and economizer temperature zones could not be made.

TIIVISTELMÄ

JAAKKO TAMMINEN: Lämmönsiirtoon pohjautuva likaantumistaipumuksen tarkastelu leijupetikattiloissa
Tampereen teknillinen yliopisto
Diplomityö, 71 sivua
Marraskuu 2017
Ympäristö- ja energiatekniikan diplomi-insinöörin koulutusohjelma
Pääaine: Energia- ja biojalostustekniikka
Tarkastaja: Yliopistonlehtori Henrik Tolvanen

Avainsanat: likaantuminen, kerrostuma, likaantumisnopeus, lämpövastus, leijupeti, lämmönsiirto, lämmönvaihdin, nuohous

Savukaasuissa kulkeutuvan lentotuhkan ainesosat voivat tarttua lämmönsiirtopinnoille ja muodostaa kerrostumia. Tämä likaantumisilmiö on yleinen muiden kattilatyyppien ohella myös leijupetikattiloissa, joissa käytettävät polttoaineet ovat usein tuhkapitoisuuden ja sen koostumuksen osalta haastavia. Tässä työssä lämmönvaihtimien likaantumisen yleiset piirteet esitellään lyhyesti, minkä lisäksi luodaan katsaus erilaisiin likaantumistaipumuksen arviointimenetelmiin, joilla on pyritty mallintamaan ja ennustamaan ilmiötä.

Työn laskennallisessa osassa testattiin lämmönsiirron analyysia likaantumisen tarkastelukeinona. Tärkeimpänä laskennallisen osan tavoitteena oli todentaa tämän lämmönsiirtomenetelmän soveltuvuus täysikokoisten polttokattiloiden likaantumistarkasteluun tekemällä jälkikäteistarkastelua vanhalla mittausdatalla. Referenssinä pidetyn puhtaan tilan kokonaislämmönsiirtokerrointa verrattiin prosessiarvoista lasketuun hetkellisen ajotilanteen kertoimeen, mistä johdettiin lukuarvo muodostuneen kerrostuman lämpövastukselle. Hyödynnetyt prosessidatat valittiin aiempien mittauskampanjoiden ajoilta. Lasketut lämpövastukset nousivat kasaantuvan kerrostuman myötä pääsääntöisesti seuraavaan nuohouspulssiin asti. Nousevien lämpövastusten aikasarjoista muodostettiin arviot likaantumisnopeudesta kullekin likaantumisvaiheelle nuohousten välissä. Valtaosin tarkasti nuohousten kanssa ajallisesti täsmänneet lämpövastusten nousuvaiheet osoittivat, että ne todella toimivat putkipintojen likaantumisen indikaattoreina.

Laskettuja lämpövastuksia ja likaantumisnopeuksia vertailtiin lisäksi automaation lokitiedoista laskettuun dataan höyrytehosta ja savukaasun paine-erosta sekä tunnettuihin polttoainesyötteen koostumustietoihin. Dataa ei ollut saatavilla kaikkia edellä mainittuja osatekijöitä varten kattavasti, mutta yksittäisiä havaintoja pystyttiin tekemään: pienet muutokset höyrytehossa eivät näyttäneet aiheuttaneen suuria muutoksia likaantumisessa, mutta savukaasun paine-eron muutos korreloi selvästi lämpövastuksen ja siten myös kerrostuman kasvun kanssa. Polttoaineseoksen vaikutus likaantumisnopeuteen puolestaan oli joissakin testipisteissä havaittavissa, mutta kauttaaltaan poltettavuudeltaan hankalien polttoaineiden ilmeneminen nopeuslukemissa ei ollut yksioikoista.

PREFACE

This Master's Thesis was done in the Energy R&D department of Valmet Technologies, a team in which I had already spent two summers before. The same team already provided me with a Bachelor's Thesis topic in late 2014, so it has been a continuous journey with great people ever since. I'd like to thank employees at the R&D department for all the support and good moments. I also thank people at the product teams for precise answers to my questions and all the fun coffee breaks.

My greatest gratitude goes inevitably to company-side supervisor of the thesis, Merja Hedman, who was my main source of support both in the thesis and in most of other work tasks that I did as side projects throughout the year, until her changeover to a new position. Combination of professionalism and casual attitude always made working with her effortless and pleasant.

For all the help, I also thank Pauli Haukka, who created the in-house tool and thus had an integral role in success of the computational part, Ville Ylä-Outinen, who was always willing to help me with calculation details and Niklas Engblom for sharing his thoughts in various stages of the work. Competence team manager Sonja Enestam I thank for giving me this great opportunity – and ensuring that I always had the required assistance from others.

Despite the extensive support I received at Valmet, I am equally thankful to my examiner Henrik Tolvanen for very constructive feedback on the contents and result presentation style. Henrik's academic way of looking at the work was fundamental in reaching an acceptable outcome.

Finally, I want to thank my parents, sister and friends for supporting me through my studies and this thesis.

Tampere, 17.11.2017

Jaakko Tamminen

TABLE OF CONTENTS

TERMS AND ABBREVIATIONS

ASTM	American Society for Testing and Materials
BFB	Bubbling fluidized bed
CFB	Circulating fluidized bed
CFD	Computational fluid dynamics
CO_2	Carbon dioxide
DCS	Distributed control system
DIN	Deutsches Institut für Normung
EN	European Standard
FACT	Facility for the Analysis of Chemical Thermodynamics
FB	Fluidized bed
LMTD	Logarithmic mean temperature difference
MSW	Municipal solid waste
NTU	Number of transfer units
PC	Pulverized coal
PPMCC	Pearson product-moment correlation coefficient
PSH	Primary superheater
RDF	Refuse derived fuel
SEM	Scanning electron microscopy
SRF	Solid recovered fuel
SSH	Secondary superheater

A	area	[m^2]
a.r.	as received (fuel content)	[-]
AFI	ash fusion index	[-]
C	heat capacity flow	[W/K]
c_p	specific heat capacity	[J/kgK]
d.a.f.	dry ash free (fuel content)	[-]
d.s.	dry substance (fuel content)	[-]
E-%	energy content percent	[-]
F_u	a fouling index	[-]
FT	flow temperature	[°C]
HT	hemispherical temperature	[°C]
IDT	initial deformation temperature	[°C]
m	mass	[kg]
r	thermal resistance	[m^2K/W]
$r_{s.a.}$	steam power adjusted thermal resistance	[m^2K/W]
$R_{B/A}$	base-to-acid ratio, a fouling index	[-]
R_c	capacity ratio	[-]
R_P	a phosphorus-acknowledging fouling index	[-]
R_s	a slagging index	[-]
RCBU	rate of calculated build-up	[m^2K/W per 10 min]
ST	spherical or softening temperature	[°C]
U	heat transfer coefficient	[W/ m^2K]
U_{mf}	minimum fluidization velocity	[m/s]
wt-%	weight percent	[-]

ε	effectiveness factor	[-]
ρ	density	[kg/m^3]

1. INTRODUCTION

The global goal to mitigate effects of the climate change requires solid actions to decrease greenhouse gas emissions. Electricity and heat generation is the most significant polluting economic activity; in EU alone, greenhouse gas emissions of over 1 200 million tonnes of CO_2 equivalents were caused by electricity, gas, steam and air conditioning supply in 2013 [18, p. 157]. Majority of the primary energy production relies on fossil fuels, and nearly half of net electricity is generated by combustion in EU [18, pp. 177–180]. Therefore, despite the role of combustible fuels in total electricity generation is decreasing, actions must be done to reduce emissions from large-scale combustion in order to meet the overall climate change prevention targets.

Despite somewhat conflicting views, biomass and waste fuels are often considered to have a neutral net effect on CO_2 emissions, so the shift in power boiler fuel selection from coal to them is a notable way to reduce the climate effects of power generation. Pulverized combustion, which is widely used for coal, cannot easily be utilized for these renewable fuels, because it requires substantial preparation of the fuel feed [56, p. 222]. Fluidized bed combustion is also more flexible to large variation in fuel composition and ash content, whereas a PC boiler could be in trouble with such feed heterogeneity [7, p. 10]. Development of fluidized bed (FB) boilers has solved many issues related to biomass combustion or waste incineration, but certain harmful phenomena are more or less unavoidable in FB boilers too. Slagging and fouling of heat exchange surfaces are examples of these issues. Although these problems are present in other boiler types as well, the objective to fire increasingly challenging fuels in FB boilers underlines the research importance specifically in these boilers.

This thesis focuses on the fouling taking place on convective heat exchangers of fluidized bed boilers. Theoretical background of the phenomenon is discussed, with attention paid to the process of a fly ash particle releasing from char, transporting onto the tube surface and contributing to the formation of a durable deposit. Earlier research conducted either to evaluate the fouling tendency or to validate the occurrence in the first place is reviewed briefly. Research focus has been on deposition analysis from chemical point of view [57], [59], [60] or modelling the fouling phenomenon theoretically or in small-scale examinations [41], [42], [44], [58], [66]. The heat transfer approach used in this thesis is known [2], [38], [45], [47], but the focus here is on statistical analysis and correlation study with operational parameters, instead of using the heat transfer results for a theoretical model verification or soot blowing optimization. Moreover, the scope here consists entirely of large-scale FB boilers and actual measurement data from them.

Primary research topic to be addressed in the computational part is to examine the fouling phenomenon by basic heat exchange calculations and to review the applicability of this method in fluidized bed boilers. Data from earlier measurement campaigns will be used for retrospective examination. Following research questions will be discussed:

- *Is heat transfer examination an applicable method to examine fouling of heat exchangers in fluidized bed boilers?*
- *How can heat transfer calculations be formulated into fouling rate estimations?*
- *What are the main operational parameters affecting fouling in FB boilers?*
- *What is the direction of causality and strength of correlation between the calculated heat transfer values and the selected operational parameters?*
- *What kind of relations do the calculated fouling rates pose between different temperature zones within each boiler, between different evaluated boilers, or with other rate determinations?*

The research questions are addressed to in the results and discussion section in Chapter 5. Primary target is to assess the method applicability; secondary goal is to have a look at the parameter correlations and minor attention is paid to boiler-to-boiler comparisons and reflection against other type of fouling rate determinations from the original measurement campaigns.

2. FLUIDIZED BED BOILERS

Fluidized bed combustion gained major development interest in the 1960s and 1970s. Since then it has become one of the leading technologies especially for biomass combustion. The diversity of applicable solid fuels combined with high combustion efficiency make fluidized bed boilers an appealing choice for combustion of challenging and varying fuel mixtures. Fluidized bed combustion generally requires only moderate pre-handling of the fuel and results in considerably smaller NOx emissions, comparing with pulverized combustion (PC), because furnace temperatures in fluidized bed boilers normally stay below nitric oxide formation limits [7, p. 12]. However, the diversity of fuel options comes with consequences of its own. The aim of this thesis is to get insight on fouling phenomenon, which is one of the major challenges that especially fuels that are rich in alkalis or have otherwise challenging characteristics may induce in fluidized bed boilers. [50, p. 490], [56, pp. 263–270]

2.1 Operational principle of a fluidized bed boiler

A fluidized bed is based on solid and inert material that behaves like a fluid. This is achieved by placing a well-controlled air flow go upwards through the bed material. Air mass flow and velocity determine the fluidization state of the bed via pressure loss alteration: for a fixed bed to become fluidized, the pressure loss of the air flowing through the bed must be at least equal to the hydrostatic pressure of the bed. Different gas velocities result in specific fluidization regimes that can roughly be sorted into four types, which are illustrated in Figure 1. After a specific minimum fluidization velocity, movement between the solids begins to occur and with further increase in gas velocity the surface layer of the bed begins to bubble. This is the operational state of bubbling fluidized bed (BFB) reactors.

The fluidization of the bed becomes more turbulent with increasing fluidizing gas velocity and the bubbling phenomenon disappears after a certain terminal velocity is reached. In extreme case the movement can be described as pneumatic transport, in which the solid particle distribution is almost equal everywhere in the boiler. Between pneumatic transport and turbulent flow patterns the ideal conditions for a circulating fluidized bed reactor (CFB) can be found. CFB reactor requires a cyclone structure to separate the solid particles from the flowing gas, whereas a BFB reactor relies on good control of the bubbling phenomenon, ensuring the material exiting the furnace to be almost entirely in gaseous form. [13, p. 8], [50, pp. 491–493]

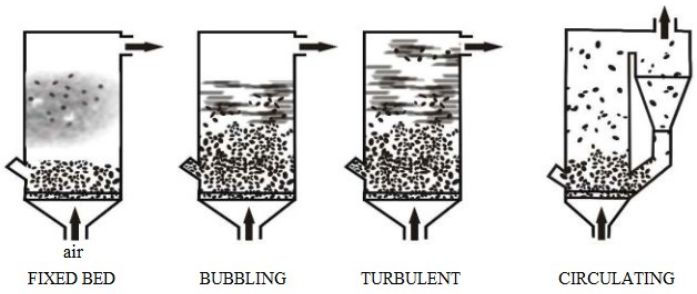

Figure 1. *Flow regimes in different fluidization states* [51]

Another significant factor on the fluidization besides the fluidizing gas velocity is the particle size distribution and the density of the bed. According to Geldart [27], the bed particles can be classified in four types by the effect of their physical characteristics on the overall fluidizability of the bed. Particles of type A have low average diameter and density (ρ < 1400 kg/m^3) and the fluidization is rather stable and the forming bubbles remain small. Type B particles have larger sizes and densities than type A particles and they form bubbles right after air velocity exceeds U_{mf}, the minimum fluidization velocity. Type B is the fluidization state for sand, which is a common main constituent of the bed. Particles of type D are still larger than type B particles, which means that U_{mf} is also higher. With type D particles, the bubbling may become spouting and therefore challenging to control. Geldart's type C particles are fine powders. The cohesion of the bed consisting of type D particles - caused by considerably strong forces between the particles - makes the fluidization difficult as the gas flow through the particles is somewhat constricted. Geldart's particle classification is depicted in Figure 2, which takes both the particle size and the overall bed density into account. [13, pp. 9–11], [50, pp. 493–500]

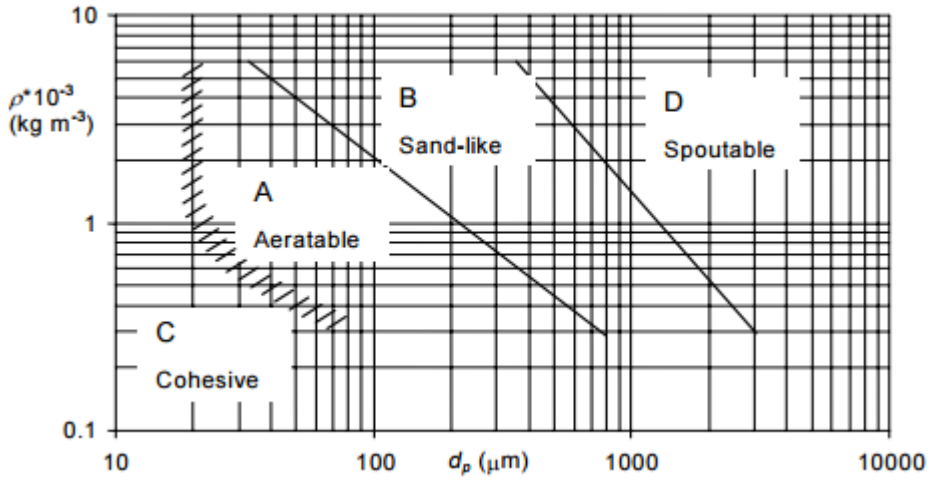

Figure 2. *Geldart's classification for bed particles* [13, p. 11]

In addition to affecting the fluid dynamics of the bed, the bed particle type also affects the heat transfer and the combustion reactions and therefore on the resulting flue gas that eventually causes the slagging and fouling issues on the heat transfer tubes and walls. The

operational differences of bubbling and circulating fluidized beds have led to distinguishable fuel-related advantages for these technologies: the more effective interaction between the bed and fuel particles enables more variable fuel selection for CFB boilers, but the conditions of a BFB boilers might favor steadier combustion for fuels of higher moisture content. However, a well-designed CFB boiler can be fired with considerably moist fuels as well. Bed material quality is crucial with practically all fuels in both boiler types nevertheless. [50, pp. 490–491]

2.2 Combustion process of solid fuels

Combustion of a solid fuel particle can be divided into a few main stages. The first of these is heating and drying. Since sufficient temperature is one of the three fundamental requirements of a combustion phenomenon, along with the fuel material and adequate amount of oxygen, a fast heating process of the fuel material is vital for reaching a high combustion efficiency. The fluidized bed heats the fuel particle very quickly, because the proportional amount of entering fuel mass flow is only a few per cents of the total solids mass in the furnace – the rest being hot bed material [7, p. 103].

Drying of a moist fuel particle takes place practically simultaneously besides heating up. Depending on the particle combustion method, drying can occur either on the surface of a shrinking particle or by simultaneous volatilization of the water content everywhere in the particle. Nevertheless of the method, the high temperature results in quick evaporation of water. [50, pp. 186–189]

Heating and drying are followed or partially taking place along with pyrolysis. Pyrolysis is thermal decomposition of the solid fuel content into volatile matter. The initial ignition happens on the volatile particles. The fragmentation of the fuel particle may happen in multiple stages; first for the original particle as primary fragmentation and then for the residual char particles as secondary fragmentation [7, p. 104], [46, pp. 232–236]. Ignition and combustion of the volatiles overlap with the pyrolysis process, as the volatiles burn while more matter volatilizes of the solid particle. According to Saastamoinen, the overall yield of volatiles vary by used fuels, being about 80 wt-% of dry solids matter for woody fuels, 60-70 % for peat and 10-40 % for coals [50, p. 193].

The devolatilization and combustion of volatiles take a considerable amount of time, and despite the fluidized bed enables efficient heat transfer between the bed and the fuel particles, the process is slower than, for example, in pulverized coal combustion [46, p. 213]. It is also noteworthy that the release rates of the volatiles vary by releasing chemical compounds. As an overall result, the total time of devolatilization and volatile combustion can be stated to depend heavily on the initial fuel particle size and the temperature of the bed [7, p. 106].

After the devolatilization and volatiles combustion, a char particle is what remains. The combustion reactions for char are even slower than for volatiles, thus giving the challenge of adequate residence time especially for bubbling fluidized beds. Char combustion is determined by chemical kinetics and oxygen diffusion to the surface and inner parts of the porous char particle. Pore and external diffusion have been estimated to be the major factors controlling the char combustion rates in both CFB and BFB furnaces under regular operation. Char combustion controlled by kinetic rate occurs mostly in lower temperature conditions. Basu divides char combustion into stages of oxygen transportation to the particle surface and the reactions between carbon and oxygen on the surface [7, p. 108]. Despite char combustion being a process of high complexity, the main overall combustion reactions may be simplified as exothermic formations of carbon dioxide and carbon monoxide:

$$C + O_2 \rightarrow CO_2, \;\; \Delta H_{reaction} = -394\ kJ$$

$$C + \frac{1}{2}O_2 \rightarrow CO, \;\; \Delta H_{reaction} = -111\ kJ$$

A char particle often will not complete combustion as a single piece. As mentioned before, secondary fragmentation caused by weakening of the particle in the combustion process might occur. Char particles might also separate into smaller fragments by mechanical attrition with other particles. This phenomenon is especially significant in circulating fluidized beds, where the particle velocities are relatively high. [7, pp. 107–110], [46, pp. 286–287], [50, pp. 202–205], [70, p. 395]

2.2.1 Combustion characteristics in fluidized bed boilers

Although the basic idea of efficient heat transfer between bed and fuel particles in fluidized bed combustion is present in both bubbling and circulating FB boilers, there are some distinctive characteristics to consider between these two boiler types. Special focus on combustion efficiency must be had when designing a furnace operating on BFB technique, as the risk of unburned carbons and CO occurring is more prevailing with BFB than with CFB. To ensure a high combustion efficiency in bubbling fluidized bed furnaces too, Basu and Oka suggest to pay attention to several factors [7, pp. 120–121], [46, pp. 403–408]. To a certain extent, an increase in bed height participates in providing a longer residence time of the fuel particles in the furnace. Recirculation of unburnt solids, utilization of secondary air injection and extended freeboard height mostly help finalize the combustion of unburnt particles in the upper area of the furnace. Feeding the fuel underbed instead of over-bed would, according to Basu [7, p. 120], give a higher overall combustion efficiency, but it also sets a requirement of smaller particle size for the fuel feed.

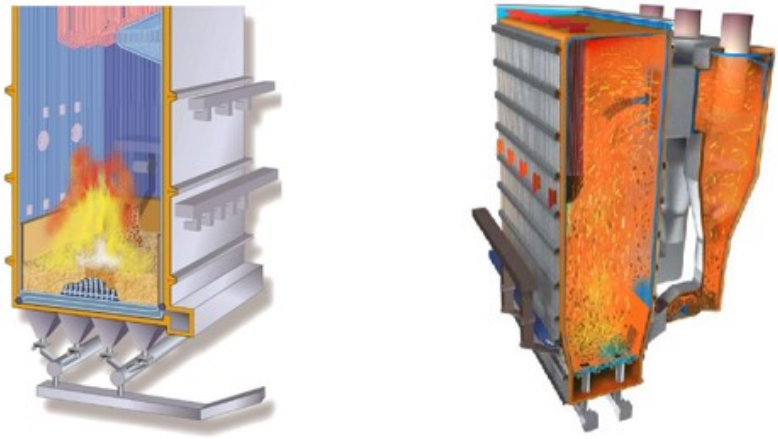

Figure 3. *Bubbling fluidized bed (BFB) furnace (left) and circulating fluidized bed (CFB) boiler (right)* [17], [36]

Figure 3 illustrates the main differences between the two boiler types combustion-wise. The bed and freeboard height are rather irrelevant terms for discussion of combustion in a CFB boiler, which relies on a looping flow of solid particles through the furnace, the cyclone and the loop seal. The cyclone is used to separate the solid particles from the flue gas. Collection efficiency varies by the particle size, being mostly over 99 % [7, pp. 394–399], [50, p. 517]. The smallest of the solid particles that might escape the cyclone to the second pass of the boiler are fly ash constituents, which in turn are major factors in the fouling phenomenon that shall be discussed later. Under the cylindrical cyclone in Figure 3 is the loop seal, which prevents gaseous combustible particles from flowing backwards to the section where pressure is lower than in the furnace. Thus, the loop seal ensures that only the circulating solids participate in the full loop of the CFB boiler flow cycle.

In terms of the zones where combustion takes place in it, the boiler can be divided into three sections: lower and upper zones in the furnace and the cyclone. Since the gas velocity of a CFB boiler is below the pneumatic transport regime, the highest concentration of solid particles is found in the lower zone. Most of the combustion happens in the upper zone though, as the secondary air inlets provide better conditions for combustion of the volatiles there. The solids in the furnace specifically form a cycle of their own, as the center parts of the furnace has smaller solids density than the areas near the walls. This is because the gas-solid suspension flows rapidly upwards towards the cyclone, utilizing the open space in the center of the furnace, and then clusters of solid matter flow downwards along the furnace walls. [7, p. 122], [50, p. 505]

Temperature of the fluidized bed is an integral characteristic of the whole FB combustion process. While the gas temperature in pulverized coal combustion may reach 1600 °C, a fluidized bed usually operates in the range of 800-900 °C – although the freeboard temperature in a BFB furnace may be considerably higher than the bed temperature. The relatively low combustion temperature in the fluidized bed increases the risk of unburnt carbons escaping the furnace in fly ash, but it is a necessity to stay under 900 °C to prevent

ash from melting. Fusion of ash can cause severe sintering issue in the bed, weakening the fluidization. Comparing with pulverized coal firing, the lower combustion temperature of a FB boiler also reduces formation of NO_x emissions and enables optimal conditions for sulfur capturing through sulfating reactions. Hardly any combustion temperature is optimal for the reduction of all emissions though, as the formation of N_2O reduces with increasing temperature, for example. However, the moderate temperature inhibits vaporization of alkali metals, which can be found in significant amounts especially when the fuel is biomass or waste. [7, pp. 126–127], [46, pp. 148–149], [56, p. 254]

2.3 Heat exchange surfaces in fluidized bed boilers

A common combustor boiler of any type relies on heating water through heat surfaces, using the heat content of the flue gas and also the radiant heat of the combustion process in some cases. Fire-side slagging and fouling phenomena take place on the outer surfaces of these heat exchange tubes. Furnaces of boilers, including those of fluidized bed combustors, handle most of the boiling phase change of the water via heat delivering membrane walls or other tube arrangements and these are where slagging takes place. The conventional individual heat transfer elements that are more exposed to fouling include superheater, reheater, boiler bank (also known as generating bank), economizer and air preheater [52, p. 203]. A schematic side view of a CFB boiler in Figure 4 shows an example of how these heat exchangers can be placed in a boiler. All examination in the computational part of this thesis focuses solely on superheaters and economizers in the convective pass, however.

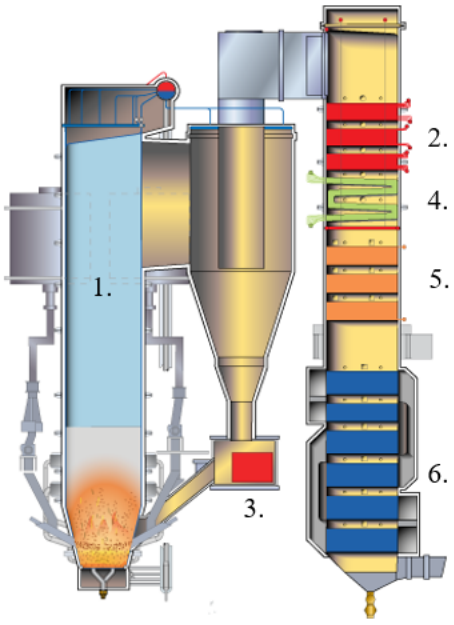

1. Furnace wall tubes
2. Primary and secondary superheater
3. Tertiary superheater
4. Boiler bank
5. Economizer
6. Air preheater

Figure 4 *Main heat exchange surfaces in a CFB boiler* [62]

Superheater is a heat exchanger that further heats the saturated team, generated in the wall tubes, into dry steam. The aim of this is to increase the enthalpy of the steam before it

enters the turbine. Superheaters can be in the convective pass, at the top section of the furnace in BFB boilers or in the loop seals of CFB boilers and based on the design, they can have various tube arrangements and flow configurations. In all the boilers examined in the experimental part of this thesis, superheaters are divided in primary, secondary and tertiary sections, based on rising steam enthalpies by increasing temperatures and mass flows. The evaluated boilers mostly contain water spray injections in between the superheating stages to increase the enthalpy effectively. [52, pp. 212–217], [65]

Reheaters are used practically for the same purpose as superheaters. Reheaters superheat the steam for intermediate- and low-pressure parts of the turbine in power plants where such division in the turbine is used. Lower steam pressures allow thinner tubes and therefore a smaller design for reheaters than what is needed for the superheaters generating the main steam. However, reheaters are not used in the FB boilers studied in the experimental part here. [52, p. 217], [65]

Boiler bank is a supplement to the evaporating wall tubes placed in the convective pass. By design it is an individual element of tubes like a superheater, reheater, economizer or an air preheater, the difference being that the last-mentioned are all used for changing temperatures of the cool-side media whereas boiler bank mainly evaporates the water into saturated steam. In addition to furnace walls and boiler banks, evaporating tube elements can also be found in the bed zone in FB boilers, like the loop seal superheater mentioned earlier. [52, p. 218]

Before entering the steam drum that feeds water to the evaporating wall tubes and boiler bank elements, the feedwater is preheated in a heat exchanger by the flue gas. This heat exchanger is called economizer. Low temperatures in both the flue gas and water sides of economizers result in the need of considerable tube surface area as opposed to superheaters. On the other hand, less severe fouling and abrasion phenomena enable the introduction of finned tubes in some economizers, thus enhancing heat exchange and compensating for the lower temperature ranges. [52, pp. 133–134]

Tubular recuperative air preheaters are usually the last heat exchanger elements in the convective pass of the boiler before flue gas cleaning or other air preheaters. Tube-based air preheaters are simple by structure but like economizers, they require substantial space in the convective duct because of low heat capacities in temperature ranges involved of both, the flue gas and the combustion air. Tubular air preheaters are also prone to dew-point corrosion occurring in cool temperatures, which forces the flue gas outlet temperature from the convective pass to be higher than what would thermodynamically be the most efficient design target value. [52, pp. 7–8, 220]

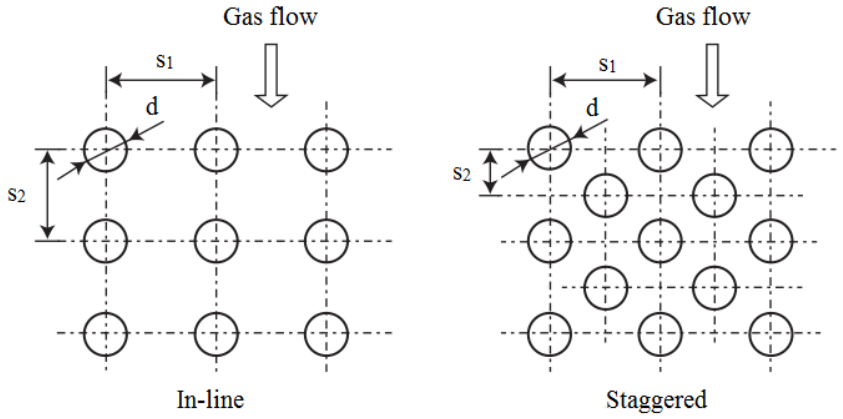

Figure 5. *Tube arrangements in boiler heat exchangers* [52, p. 217]

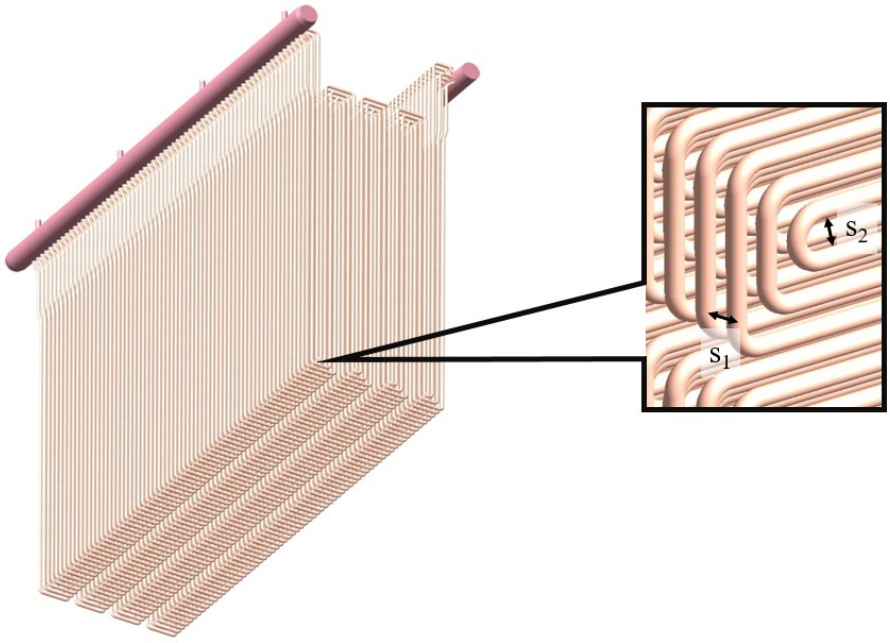

Figure 6 *Depiction of tube pitches in a heat exchanger* [31]

Figure 5 shows two main types of tube arrangements of the heat exchangers presented above. The in-line arrangement is further illustrated in Figure 6 for a complete convective pass heat exchanger. While the staggered form of tube elements is more compact and enables more effective heat transfer from the flue gas, it is more vulnerable to fouling. In-line arrangement keeps the flue gas flow more laminar, which should result in lesser fouling. Other related physical factors affecting the flue gas flow pattern and fouling are the transverse and longitudinal pitches between the tubes, presented in figures 5 and 6 as s_1 and s_2, respectively. The relationship between the transverse and longitudinal pitches varies, as the pitches are not necessarily as equal as the layout in Figure 5 suggests. In any case, a tight arrangement can enhance the fouling effect by restraining the flue gas flow. [52, p. 217]

2.4 Common fuels used in fluidized bed boilers

A wide selection of solid fuels can be fired in fluidized bed boilers, including fossil fuels of rather low quality, woody matter, different kinds of recovered feeds such as sludges and municipal solid waste (MSW), and agricultural residues [7, pp. 10–11]. While being a key advantage of FB combustion over other combustion technologies, this fuel variety is also challenging from boiler design point of view. Basic characteristics of fossil fuels, woody biomass, agriculture-based fuels, and recovered fuels including wastes and sludges are presented in this chapter to gain conception of the common fuels in FB boilers.

2.4.1 Fossil fuels

Coal was the largest source of electricity generation worldwide in 2012, accounting for 41 %, or 9 204 TWh of the global production [33, p. 208]. Pulverized coal combustion is the principal form of combustion of coal, but fluidized bed combustion offers multiple previously mentioned advantages over PC combustion, such as possibilities of efficient sulfur reduction and reduced NO_x formation. However, these advantages might not be enough to make fluidized bed combustion superior over PC combustion, when coal of good quality is the only fuel. The benefit of FB combustion comes from the superior ability of cofiring of coal and biomass. Regardless of this, coal is often the primary fuel in CFB boilers too and its current importance should not be neglected. [26, p. 912], [34, pp. 49–51]

Typical classification of coals depends on the volatile content in them, which practically compares to the duration of the matter having being decomposed in the rock sediments. Heating value and thus the overall quality of the coal increases with decreasing volatile matter content, which can be seen in Table 1. Coal fuels are generally ranked by increasing quality in lignite, subbituminous, bituminous, semianthracite and anthracite coals [21, p. 169]. Examples of characteristic data of coals using slightly different classification, compiled by Spliethoff [56, pp. 17–18], is shown in Table 1.

The data in Table 1 gives an idea of what the key differences between the coal ranks are, besides the varying amount of volatile matter. Ash and water contents decrease along decreasing volatile matter. This not only makes the combustion more efficient but also reduces the problematic issues related to ash formation, such as slagging and fouling. Spliethoff's original data also indicates a strong tendency of increasing carbon content by declining volatile matter. The high carbon contents in the dry ash-free substance of high rank coals is paralleled to relatively low oxygen shares. [56, pp. 17–18]

Table 1. *Characteristic values of different coal ranks* [56, pp. 17–18]

Coal rank	Volatiles (wt-% d.a.f)	Ash (wt-% a.r.)	Moisture (wt-% a.r.)	Lower heating value (MJ/kg, a.r.)
Peat	68.5-69.6	1.5-22.0	40.0-55.0	7.3-7.9
Hard brown coal	44.5-56.0	4.0-35.0	2.0-35.0	10.0-27.6
High-volatile bituminous coal	33.7-41.5	4.6-9.0	3.0-13.8	26.3-28.9
Anthracite	4.0-7.7	5.0-7.0	3.0-5.7	30.0-31.4

The fuel flexibility of FB combustion enables usage of some byproducts of oil refining industry. One of these is petroleum coke, which is a residue of thermal cracking process in oil refineries. Petroleum coke has high carbon content but also often harmfully high sulfur share of the dry substance and this makes it an unappealing fuel option for pulverized coal combustors. A review conducted by Chen and Lu [10] shows that with the right sorbent material, combustion in a CFB boiler can be feasible though, and thus petroleum coke is a fine example of the superior fuel handling capabilities of FB combustion over conventional technologies. In this particular case of fuel, added limestone sorbent reduces NO_x emissions as well, even though typically limestone is a catalyst in some NO_x formation reactions. [3, p. 242], [7, p. 159], [10, pp. 204–206]

2.4.2 Woody biomass

Woody matter is the main source of solid biomass fuels and most of it is consumed in traditional forms, including fuel wood and charcoal, for example [54, p. 287]. Chips and pellets represent modern methods of woody fuel pre-handling. According to the EN standard 14961-1, solid woody matter can be separated into whole trees, stem wood, stumps and roots, logging residues, bark, segregated wood and various blends of these all [28, p. 23]. Chemically treated waste wood is usually considered as waste fuel instead of pure woody biomass.

Chemical properties of the woody matter are significantly affected by which part of the tree the material is processed from. The degree of implemented pre-handling on the material also influences, for example, the moisture content. Mean values for some key characteristics of woody biomass fuels, compiled from ECN fuel database [16], can be found in Table 2. As the table indicates, the heating values of woody biomass are considerably lower than those of high quality coals, but ash content on the other hand is also very low

in virgin wood material. Besides direct energy use of virgin wood, bark or residual woody matter after appropriate mechanical pre-handling, woody fuels can also be residues of pulp and paper industry, such as bark or sawdust from the bark stripping process in a pulp mill. Therefore, woody biomass fuels have important roles in the fuel mixtures of power boilers especially associated with pulp and paper plants.

Table 2. *Characteristic values of woody biomass* [16]

Fuel type	Moisture (wt-% a.r.)	Ash (wt-% d.s.)	Carbon (wt-% d.s.)	Oxygen (wt-% d.s.)	Chlorine (wt-% d.s.)	Lower heating value (MJ/kg d.s.)
Wood (birch, pine and spruce)	11.09	0.65	50.53	42.43	0.016	18.73
Bark	14.12	3.17	52.18	38.71	0.015	19.10
Forest residue	29.37	3.11	50.60	40.01	0.021	19.18

The use of virgin wood or pulp and paper industry residues for combustion varies greatly by area. In Europe and North America wood is mostly used as round wood for further refining, whereas in South America, Asia and Africa it is mostly used as fuel. A substantial share of the combustion in the latter is traditional small scale activity, however. For instance in Germany on the other hand, majority of the woody biomass that could be a part of energy production feedstock is already utilized in some other way, which limits the combustion capabilities of the wood matter, be it traditional small scale or modern large scale application. [23, p. 24], [56, pp. 34–35]

2.4.3 Agricultural biomass and energy crops

In Sweden and Finland, for instance, the well-established forest industry has led to relatively high utilized yields of wood matter from forests and to usage of low-grade woody residues as fuels in boilers. Worldwide though in warmer countries, energy crops have competitively potential production figures for combustion purposes as well. Particularly strong growth is expected in the favorable climate conditions of Africa and South America. In Asia, great potential can be seen for herbaceous biomass too. Agricultural biomass - as it is categorized here at least - is a broad class for all crops and residues related to agriculture and herbaceous plants. Examples of agricultural biomass fuels are presented in Table 3. [56, pp. 32–34]

The EN 14961-1 standard acknowledges several agricultural biomass types, including e.g. cereal crops, grasses, oil seed crops, herbaceous residues, fruits, blends and residues related to processing of plants in each of these segments. Despite being classified under

the loosely defined agricultural biomass class, perennial energy crops actually produce woody matter or, in other words, they have rather high lignocellulose content. Good examples of these are willow and poplar (seen also in Table 3), whose subspecies can thrive even in relatively cold climate conditions.

Table 3. *Characteristic values of agricultural fuels and energy crops* [16]

Fuel species	Moisture (wt-% a.r.)	Ash (wt-% d.s.)	Carbon (wt-% d.s.)	Oxygen (wt-% d.s.)	Chlorine (wt-% d.s.)	Lower heating value (MJ/kg, d.s.)
Wheat straw	10.17	6.36	45.80	41.33	0.401	16.99
Rice husk	10.04	18.79	38.70	37.18	0.104	13.85
Reed canary grass	14.21	7.69	45.26	40.59	0.086	16.67
Willow	16.42	1.82	48.87	42.78	0.015	18.06
Poplar	9.9	1.13	49.35	43.24	0.041	18.57

Constitutive differences in the chemical compositions between energy crops and herbaceous plants exist, as Table 3 indicates – and these differences highlight the better combustibility of energy crops. However, it should be perceived that energy crops are obviously cultivated for energy production purposes, whereas wheat straw, rice husk and other food crop residues are secondary products from food processing industry. Therefore, regarding their primary purpose, food crops preferably contain nutritive substances like alkalis that are important in food but possibly harmful in combustors. In Table 3, special attention should be paid to chlorine content, which is a highly unwanted component to be found along with alkali metals. Comparisons between Tables 2 and 3 point out that the Cl content of the worst agricultural fuels can be several magnitudes higher than those of woody fuels. [6, pp. 278–281, 392–396], [23, pp. 27–28], [28, p. 25,27,134]

2.4.4 Waste fuels

On average in the European Union, 475 kilograms of municipal waste (MSW) per capita was generated in 2014 [19]. When all sources except mineral wastes are taken into account, the figure for year 2014 was 1,8 tons per capita [20]. Despite the large range in waste generation among the EU countries, the agreed conclusion is that actions should be done to prevent generation of waste and it should be the first priority in waste management. The second priority is to improve material and energy recovery of the generated waste. The aim of recycling is to separate the recoverable matter from bulky waste and the rest is disposed of by landfilling or waste incineration. The MSW ending up to be

incinerated is more mixed than the easily recoverable matter. Even so, it is generally pre-handled further in waste treatment plants into refuse derived fuel (RDF) or solid recovered fuel (SRF) before combustion to ensure sufficiently homogenous consistency for the fuel feed. The nominal difference between RDF and SRF wastes is external certification of the material composition, meaning that SRF fuels are more strictly defined by composition. [37, pp. 75, 79], [56, pp. 35–36]

Accepted waste material groups for SRF raw material are recycled paper, wood and cardboard, textiles, plastics, rubber and other fairly calorific non-hazardous wastes. The CEN-TC 343 standard sets quantitative minimum limit for the lower heating value and maximum limits for chlorine and mercury contents of the fuel mixture to get approved as SRF fuel. These limits can be found in Table 4 along with average analysis results for selected waste fuels from the ECN fuel database. Due to lack of certified SRF samples, RDF sample averages were chosen to represent general, loosely defined waste in the table. Instead of being listed under woody biomass, demolition wood is listed in Table 4 to highlight the secondary nature of combustion as a utilizing method of woody matter. Comparison of the ash and chlorine contents between Table 4 and tables Table 2 and Table 3 implies that even after the mechanical separation, reduction of impurities and metals and other pre-handling processes, the wastes are still the most challenging renewable solid fuels for combustors. [37, pp. 78–80], [56, pp. 76–78]

Table 4. *Waste fuel characteristic values and standard limits for SRF* [16], [37, p. 80]

Fuel species	Moisture (wt-% a.r.)	Ash (wt-% d.s.)	Carbon (wt-% d.s.)	Oxygen (wt-% d.s.)	Chlorine (wt-% d.s.)	Lower heating value (MJ/kg, d.s.)
CEN-TC 343 SRF Standard limits	-	-	-	-	<0.1-6.0 (a.r.)	>3.0-45.0 (a.r.)
RDF	10.04	17.03	45.53	28.31	0.555	18.80
Demolition wood	13.64	6.93	46.94	39.57	0.136	17.58
Recycled paper and cardboard	7.03	10.46	42.66	40.97	0.038	16.30
Sewage sludge	20.56	41.55	30.04	18.35	0.262	12.47

With their capability of handling relatively high moisture contents in the fuel, achieved by thoughtful design, fluidized bed boilers can incinerate certain types of sludges too. For instance, these could be pulp and paper industry residues, such as deinking sludge, or some sewage sludges. However, some sort of dewatering might be needed for efficient combusting, and even then, the sludges could only serve as secondary constituents in the

fuel mixtures, as Maier's examples from power plants in Germany suggest. As can be seen in Table 4, the ash content of an average sewage sludge is high – or almost extreme in comparison with other wastes – and its effects on the combustion need to be mitigated by careful adjustment of the proportion of the sludge in the fuel feed. [56, pp. 38–39]

2.4.5 Fuel category comparison and effect of co-combustion

A summarizing comparison of the fuel categories presented earlier is listed in Table 5. Peat, bituminous coal, wood including birch, pine, and spruce, wheat straw, and RDF were chosen to represent those categories in the table. The table shows how deviating the compositions of these materials can be, which also corresponds heavily to lower heating values of dry substance. Solid fuels of any origin consist mostly of moisture, C, H, N, O, S, Cl and ash [60, p. 10], and it is clear that increasing carbon and decreasing oxygen content are the key affecting factors on the heating value of the dry substance. Chlorine and alkali (Na + K) contents for peat and coal in Table 5 were summarized in [60].

Table 5 *Comparison of different kinds of solid fuels* [16], [56, pp. 17–18], [60, p. 10]

Fuel species	Peat	Bituminous coal (high-volatile)	Wood (birch, pine, and spruce)	Wheat straw	RDF
Moisture (wt-% d.s.)	40.0-55.0	3.0-13.8	11.1	10.2	10.0
Ash content (wt-% d.s.)	1.5-22.0	4.6-9.0	0.65	6.4	17.0
Carbon (wt-% d.s.)	57.50-58.0	81.4-85.9	50.5	45.8	45.5
Oxygen (wt-% d.s.)	33.5-34.9	6.2-10.3	42.4	41.3	28.3
Chlorine (wt-% d.s.)	0.056	0.221	0.016	0.401	0.555
Lower heating value (MJ/kg d.s.)	7.3-7.9	26.3-28.9	18.7	17.0	18.8
Alkali (Na+K, wt-%d.s.)	0.07	0.21	0.15	1.00	0.46

Chlorine and alkali metals, sodium and potassium, were included in the comparison above because of their importance in the slagging and fouling phenomena, which are further discussed in Chapter 3. Furthermore, the listed moisture content averages hide large deviation behind the figures, as the included analyses in ECN fuel database [16] labels fuels mainly by species, not by preparation stages where drying processes would be taken into

account. This should be acknowledged when interpreting the dry heating values that favor biomasses and RDF a bit in Table 5, in comparison coal and peat.

Hupa [32, p. 1313] listed a few BFB and CFB boilers and the fuels they use. Coal, waste wood, RDF, and peat are common in CFB combustion, while BFB boilers are fired usually with forest residue, bark, peat, or pulp and paper mill residual sludges. Fuel is typically crushed to a smaller size for CFB boilers than what would be required for BFB. On the other hand, BFB combustion cannot necessarily handle an equally large share of fines (< 1 mm) than CFB without consequences on combustion efficiency [52, p. 67]. Rayaprolu [52] suggests that upper fuel sizing limits for coal (although not usually fired in BFB) would be < 20 mm for over-bed-fed BFB and 6.0-8.0 mm for CFB. Overall fuel flexibility is higher in CFB anyway, even though fuel pre-handling would be more demanding with it. [52, p. 168]

Combustion of biomass and waste fuels in FB boilers is often co-combustion either with coal or between easy and challenging biomass or waste feeds. Out of all the specific challenges that biomass and waste fuels cause in FB combustion, the bed agglomeration problem especially is reduced by co-firing with coal. Sulfur in coals boosts alkali capturing into alkali sulfates, inhibiting harmful reactions of alkalis with quartz sand [7, p. 129], [12, p. 3]. Biomass and even waste fuels have typically low sulfur contents, and therefore coal co-firing not only assists in bed condition management, but reduces the SO_2 emissions compared to full coal combustion [32, p. 1314], [56, p. 459]. Combustion of challenging, alkali-rich agricultural fuels benefit from coal even more than wood, but coal use mitigation targets have led to the incentive of co-firing woody matter as the supporting fuel with agricultural feeds. This can be troublesome, however, as the joint effect of these feeds can be hard to predict [12, p. 3].

3. SLAGGING AND FOULING PHENOMENA

Problems imposed by solid biofuels and wastes in fluidized bed boilers are rather well known. Alongside bed particle agglomeration and corrosion at high or low temperatures, slagging and fouling are recognized as major operational issues by, for example, Raiko et al. [50, pp. 284–287], Spliethoff [56, pp. 377–378], Basu [7, pp. 127–130] and Bryers [9, p. 30], so the consensus on the severity of these issues is quite clear. Not all these problems can be directed solely to the use of challenging fuels, however. The chemical substances contributing to the generation of agglomerates, corrosion or slagging and fouling deposits are partially the same nevertheless.

The main separation between the terms slagging and fouling is the occurring location in the boiler. Bryers [9, p. 31] specifies slagging to be deposition that takes place in the parts of the furnace where radiation is the primary heat transfer method. Fouling refers more to deposition on heat exchanger surfaces after the furnace, or convective heat transfer area. The deposits contributing to slagging are exposed to higher temperatures than deposits in the fouling zone and this often gives them molten appearance, while deposits in the fouling parts of the boiler occur more certainly in solid phase. However, the state of the deposit depends on several factors that are discussed in paragraph 3.2. The scope of this thesis focuses on the fouling phenomenon, but by occurrence, fouling and slagging are often inseparable. Formation of the deposits is strictly related to ash formation during combustion, so it is crucial to understand the ash forming behavior first. [50, pp. 260–261, 275]

3.1 Ash formation

The basics of the combustion process of a solid fuel particle were discussed in paragraph 2.2, but no insight was given on what happens to the residual matter in char particle combustion. Ashes forming in fluidized bed combustion may be classified in bed ash, cyclone ash and fly ash in regard to the related location in the boiler, and especially the fly ash formation is important to acknowledge with biofuels of high volatile content. [35, p. 836], [56, p. 342]. Figure 7 shows the formation methods of ash components from a char particle. Similar figures are also presented by Raiko et al. [50, p. 260] and Zevenhoven [68, p. 31]. Fly ash constituents may also originate in gaseous form from combustion of volatile matter, however.

The ash particle size distribution graph in Figure 7 indicates that two separate groups of fly ash particles are formed in char combustion. The lower part in the figure represents ash formation through combustion of the fragmented char, in which the coarse fly ash with mean size of about 10 μm is a solid residue of the combustion. Ash formation

through vaporization of inorganic gases is shown in the upper part of Figure 7, pointing out the possibility of presence of major ash forming elements in gaseous form in the boiler. According to the figure though, the general pathway of these gases is to condensate and agglomerate into fine ash. Another formation route for submicron particles is through nucleation of saturated vapors into tiny nuclei, which can further coagulate into slightly bigger particles with a mean size of approximately 0.2 µm. The difference between the above-mentioned methods is the homogeneity of the particles forming the small nuclei in the uppermost process of Figure 7, compared to the more varying consistency of the product through heterogeneous condensation. Corresponding particle size distribution ranges of 0.1 - 1 µm or 0.05 – 0.5 µm for the gaseous pathway and 1 - 100 µm or 0.5 - 50 µm for the char burnout process are presented by Raiko et al. and Zevenhoven. [22, p. 295], [35, p. 836], [50, p. 260], [68, p. 31]

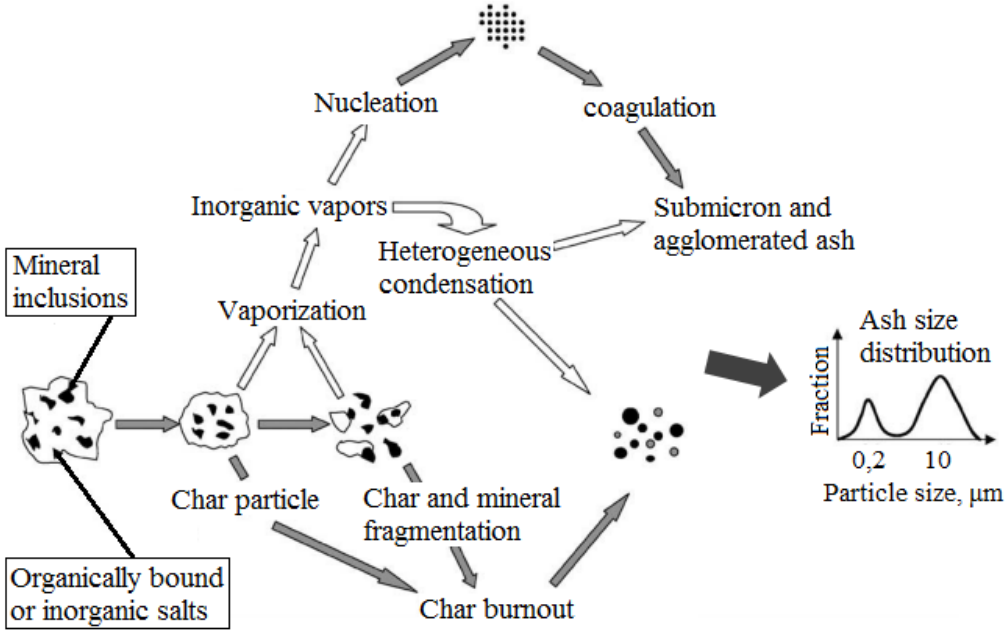

Figure 7. *Ash formation methods of char particle combustion* [35, p. 836]

Alongside with chlorine and sulfur, a few generally known major elements participate in ash formation. These are aluminum (Al), calcium (Ca), iron (Fe), potassium (K), magnesium (Mg), sodium (Na), phosphorus (P), silicon (Si) and titanium (Ti) [5]. The fractions of these elements within different solid fuels vary a lot, but some guidelines may be assumed. Typically, the ash of woody biomass has relatively high share of alkali and alkali earth metals. Agriculture-based fuels can be even higher in alkali content. As for fast-growing herbaceous biomass, peat and fossil fuels, some siliceous and ferrous compounds are common too. Aluminum is mainly found in peat and fossil fuels because of its toxicity to living plants. In general, the ash forming elements can be categorized to be present in silicate, oxide, carbonate or sulfate compounds. Another approach to define the form or origin of ash compounds is division between organically associated and mineral associated component fractions in the fuel. In biomass fuels, the ash forming compounds are

primarily related to the organic matter, whereas major element occurrence within mineral particles is more common in fossil fuels. [50, pp. 270–274], [60, p. 12], [68, p. 32]

3.2 Deposition of fly ash

The deposition of the ash on heat transfer surfaces has numerous effects on boiler design and operation. Minimization of slagging and fouling requires careful considerations of soot blowing, flue gas and steam temperatures, combustion air distribution and boiler load, for example [9, p. 32]. The fuel composition, interaction with bed particles in fluidized bed boilers and overall ash chemistry play a major role in deposition formation too. When considering the slagging and fouling effects, a few key characteristics of the deposit can be found: easiness of removal off the heat transfer surface, viscosity, effective thermal conductivity, effective emissivity and strength [68, p. 35]. These define the severity of the operational impairment that the deposits cause.

3.2.1 Ash particle transportation to the surface

Formation of a deposit demands transportation of ash particles on the heat transfer tube surface. Three main processes of transport and initial deposition are diffusion or condensation of gases, impaction and thermophoresis. Diffusion and thermophoresis are common processes for gaseous submicron particles, whereas inertial impaction is more noteworthy for large particles at least 10 µm of size. The relation between particle size and the transport mechanism results also in chemical composition differences by the occurring mechanism: Ca, Si and Al appear more frequently in the inorganic, coarse particles subjected to inertial impaction, whereas alkali chlorides and sulfates can diffuse on the tube surface more easily. Figure 8 depicts how the different deposition mechanisms affect each side of the heat exchanger tubes. [57, p. 329]

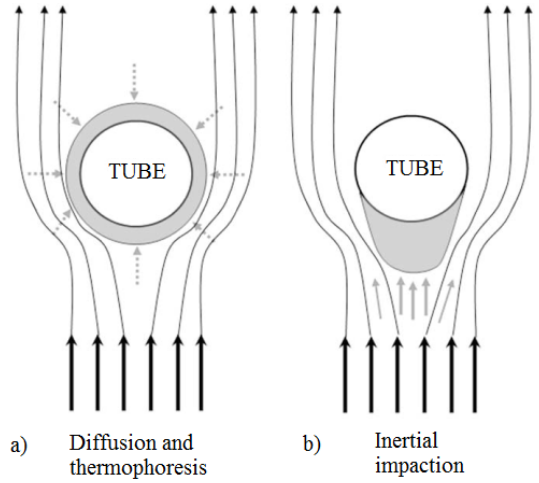

Figure 8. *Deposit transportation mechanisms onto the tube surface* [67, p. 34]

Diffusion describes the flow of particles due to a concentration gradient, which directs the flow towards the smaller concentration areas. This so-called Fick diffusion principle is supplemented by random Brown diffusion and Eddy diffusion, which represents the portion of flow turbulence in the overall diffusion phenomenon. Diffusive condensation of gaseous ash particles is particularly critical at the beginning of the deposition, as it can multiply the favorable contacting surface on the tube for following ash particles. Fick diffusion-dominated transportation is depicted in Figure 8 on the left-hand side.

Thermophoresis is particle movement towards lower temperature via imbalance of kinetic energies of particles in hot and cold environments. The hot particles have higher impact velocities than cold particles, generating net forces on particles exposed to temperature gradient. This results in opposite directions between the particle flow and the temperature gradient.

Impaction is the most prominent deposition method after initial deposit layer formation via diffusion and thermophoresis. It is the process of relatively large fly ash particles hitting the tube surface because their size hinders their ability to follow the flow streamlines that pass around the tube. The high inertia of the heavier particles can force them off the flow and make them collide with the tube and stick to the initiated deposit layer. Flue gas flow characteristics and particle and tube geometries have notable effects on the impaction deposition tendency, as for the deposition to take place, the maximum angle between the tube centerline and the particle flow line is around 50°. Therefore, deposition by inertial impaction accumulates mostly on the front side of the heat transfer tube, as Figure 8 suggests. [22, pp. 295–296], [50, pp. 245–246], [60, pp. 19–21], [68, p. 36]

Ash transportation mechanisms and flue gas flow characteristics may force to widen the spacing between tubes, if challenging biomass or waste fuel is fired [52, p. 212]. This can increase cost of the boiler via designed enlargement of the convective pass. Flue gas velocity is also a key parameter to consider when discussing ash particle transportation. Basu presents that typical convective pass flue gas velocities are 12-16 m/s in CFB boilers and 20-25 m/s in PC combustors [7, p. 301]. While a high velocity of the flue gas might decrease impaction rate, Basu and Rayaprolu emphasize how tube erosion tendency gets severely higher with increasing gas velocity, limiting the maximum sensible velocity. [7, pp. 301–302], [52, p. 186]

3.2.2 Sticking and consolidation on the surface

Contact between an ash particle and tube surface is not a guarantee of deposit formation. For ash matter to accumulate on the surface, it needs to adhere and form a hardened layer on it. The transportation methods described in the previous paragraph depend heavily on the physical features of the ash particles in the flue gas flow, but the extent of adhesion to the surface depends also on the chemical composition the ash. The stickiness can be

described as the joint effect of particle and surface temperatures, elemental particle composition and physical flow characteristics.

The influence of temperature brings forward the differences between boiler types. From deposition point of view, the lower furnace exit temperatures of fluidized bed boilers in comparison with PC combustors help with the goal of restraining fly ash fusion on the heat transfer tubes of the boiler. Molten layer of ash directly on the tube surface not only enables further deposit formation but it can trigger fast-developing high temperature corrosion of the tube material as well. It is important to understand that the ash mixture consisting of various compounds does not have a single melting point. Instead, four different temperatures are used to describe the phase change. These are initial deformation (IDT), spherical or softening (ST), hemispherical (HT) and fluid temperatures (FT). The difference between the IDT and the FT can be several hundred °C, leading to coexistence of solid and molten phases. The changes of melting ash particle shape as stated in DIN 51730 standard are depicted in Figure 9. Stickiness tendency depends rather strongly on the degree of molten matter in the ash mixture on the tube surface. This sticking induced by liquid phase content can also be accompanied by chemical reaction sintering. [50, pp. 278–284], [56, pp. 22–23]

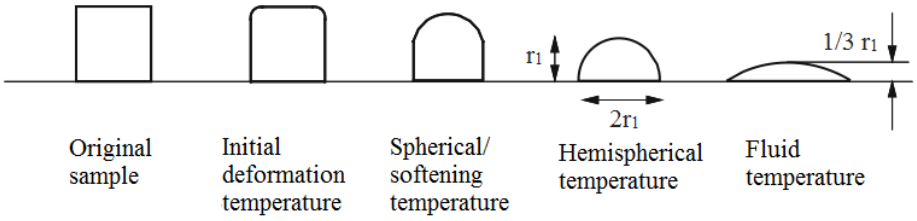

Figure 9. *Particle shapes at different ash fusion temperatures* [56, p. 22]

The ash fusion temperatures tend to be lower for ashes rich in alkali compounds, demonstrating the difficulty of dealing with ash from alkali-rich agricultural fuels, for example. Out of individual elements, Miles et al. [39] emphasize the importance of potassium, sulfur, chlorine and silicon. Potassium occurs often in organic form, resulting in potential vaporization and condensation on tube surface. Potassium compounds also contribute to lowering of ash fusion temperatures. Sulfur and chlorine act as reactants with alkali and other metals, enabling formation of sulfates and chlorides. Sulfating and carbonation reactions can harden the formed deposits and thus reduce soot blowing capabilities for fouled tubes.

The combined effect of K, S and Cl is relevant in co-combustion of different fuels: for example, woody fuels alone typically do not contain much sulfur or chlorine and rather clean combustion is possible, but combustion with sulfur- or chlorine-rich fuels raises the potential of reactions between the alkalis from the wood and S and Cl from the other fuel in the mixture. Therefore, also the fusion temperatures can be lower for fuel mixture ashes

than what the ashes of the pure fuels would demonstrate. Chlorine especially facilitates vaporization of alkalis, and this is why combustion of fuels of high alkali but low Cl content might be rather trouble-free. [39, p. 136]

Backman et al. presented that in order for the deposit to be sticky, the liquid phase content needs to be in the range of 10-70 wt-%. This critical range was found for black liquor in a recovery boiler, however, and Zevenhoven suggests that another definition for critical fusion phase is required for siliceous fuels. The initial deformation temperature of silica is considerably high at 1700 °C, but together with other oxides it can form a glass layer at temperatures much lower. The lower the viscosity, the higher is glass formation via viscous flow sintering, and alkali metals reacting with silica tend to bring the viscosity down. The result is then a layer of hardened silica glass on the tube surface, while pure silica alone could form larger particles that would more easily rebound back to the flue gas. [4], [22, p. 297], [39, pp. 136–137], [50, pp. 271, 281–283], [68, p. 37]

Forces between individual atoms can also affect the adhesion of flue gas particles on the surface. Example of these are van der Waals forces, which occur between polarized atoms and molecules. The polarization generates dipoles that make the atoms either repel or attract each other. Another example of active forces at atomic scale are electrostatic forces, which are caused by electrical surface charges on solid particles. Imbalance of charges near the tube or deposit surface can create a local electric field that generates an electrical diffusion layer for particles colliding with the surface. Electrostatics and van der Waals forces demonstrate how complex the overall adhesion and deposition mechanisms can be. [8, pp. 46–51], [60, p. 23]

3.3 Characteristics of slagging and fouling

As mentioned earlier, the term slagging is specified to refer to deposition phenomenon in the area of the furnace where radiative heat transfer is dominant. The exposure to higher temperatures in the radiative area than in the convective parts results in ash particle sticking by melting being the principal slagging method. The chemical composition of the flue gas and fly ash in it are the main contributing factors to the slagging phenomenon, but local presence of slag can also indicate that burner positioning and air distribution can be poor or that the geometrical shape of the furnace is not well optimized. Burner positioning is naturally relevant mainly in PC boiler furnaces. Because of the moderate temperature regimes in fluidized bed boilers, slagging is perhaps not a problem to the same extent in FB boilers than it can be in PC combustors or grate boilers, but a considerable issue to keep in mind nonetheless. Differences in tube element placement and bed material circulation characteristics lead to BFB furnaces being more vulnerable to slagging problems than CFB furnaces before the cyclone. [56, pp. 325–326]

Silicates are often the main compounds participating in slagging. As explained above, alkali content in silicate compounds brings viscosity down and enable ash melting at rather low temperatures. Slagging effect can also be enhanced by ferric oxides, which are abundant in pyrite, a common mineral in some coals. Finding a solid fuel that does not include significant amounts of any slagging contributors can therefore be challenging at the very least, as low alkali and silicon contents alone are not sufficient guarantees of easy slagging prevention. [9, p. 81], [50, pp. 285–286]

As described earlier, fouling is deposition in the convective part of boiler and it is characterized by relatively small amount of molten phase in the deposit, as opposed to slags in the furnaces. Even though the sticking and consolidation mechanisms discussed in Chapter 3.2.2 apply to the convective parts of boilers too, the dryness of the fouling deposits reduces the stickiness and rationalizes the use of soot blowing technology to remove the non-sticking material off the tube surface. As a result of this, particles are transported onto the tube surfaces by inertial impaction more in the convective part than in the furnace – but this does not mean that diffusion would be insignificant at all either.

Zbogar et al. [67, p. 37] divide convective pass fouling into two different sections by varying temperature fields: high temperature fouling takes place when bonding between ash particles happens by alkali silicate phases, whereas in low temperature fouling the bonding forms primarily via sulphate phase formation. A similar division logic is followed in the computational part of this thesis, where broad comparisons between two different temperature ranges are conducted.

3.4 Deposit removal

Despite the formed deposits can become rather consolidated, mechanisms to remove them are generally used as a regular part of boiler operation. Removal of the deposits not only revives heat transfer from the flue gas into the receiving medium, but also protects tube surfaces from exposure to harmful and possibly corrosive reactants found in the deposits. Zbogar et al. [67, p. 38] have divided the removal mechanisms into load changes and various cleaning systems. The latter include different kinds of soot blowers, such as sonic wave or steam blowers and pneumatic knocking systems, which are applicable in the convective part, reducing fouling effects. Water cannons and air pressure wave explosions are techniques that can be used in the furnaces to prevent slag build-up, respectively. [29, p. 140]

Zbogar et al. show up that the ash deposit can fall off a surface also naturally by various mechanisms. These include erosion, shedding by gravitational force, liquid slag flow and tension-related removal thermally or mechanically. Liquid slag flow requires a considerable share of the deposit to be in liquid phase, implying the phenomenon to take place mainly in furnaces. Erosion and gravity shedding can take place in the opposite case, where the deposit mainly consists of loose dust. Forced removal by soot blowing and load

changes contribute to mechanical and thermal stress alteration mechanisms, with steam soot blowing being a combination of both of these tension-related types. The proportional effect of all mentioned methods depends on the stickiness and consolidation characteristics of the formed deposits. [67, p. 39]

Surface temperature has a mixed role in the deposit removability. The higher the tube surface temperature is, the higher is also the chance that a portion of the ash deposit is in molten phase, which might increase deposit stickiness - but also reduce tensile strength. Zbogar et al. suggest that required soot blowing jet pressure increases by increasing temperature until a certain limit, after which the reducing deposit strength and possible increase in porosity result in rapid decline in required jet pressure [67, p. 52]. This view of decreasing removal efficiency by increasing material temperature is backed by Zhou et al. [69].

Graube et al. [29, p. 144] had a somewhat different approach on the question of the relation between deposit removability and material temperature. They emphasized the effect of temperature gradient in the soot blowing utilizing thermal tension; a high temperature difference between the soot blowing medium and the tube should increase the deposit removability, in the case that the deposit strength is in relation to temperature changes. In other words, deposit removal in hot zone should be more effective than in colder parts, because of the higher temperature gradient. Actual influence of temperature might be somewhere between these two somewhat conflicting perspectives, depending on the stickiness characteristics of the ash and the sensitivity to thermal shock soot blowing.

Zbogar's et al. interpretation of required soot blowing jet pressure can be seen in Frandsen's review too: if the material temperature is high enough, e.g. 500 °C, it is possible that no sensible jet pressure is large enough to break the deposit layer [22, p. 286]. Graube et al. reached a similar conclusion, although their statement had a distinct perspective. Their results indicated that increasing momentum of the jet enhances the deposit removal a bit at surface temperature of 540 °C, whereas similar relation cannot be seen at more moderate temperature of 325 °C [29, p. 145]. A general and agreed conclusion was that the role of thermal shock is normally greater than the mechanical shock of the soot blowing jet, and that the temperature of the deposit, its composition and its structure are very integral factors in assessing the overall removability.

3.5 Research on fouling tendency examination and prediction

As combustion of challenging biomass and waste fuels is increasingly common especially in fluidized bed boilers, the ability to predict the tendency of slagging and fouling phenomena becomes more important. However, the mechanisms of initial deposition and deposit build-up are manifold, as the overview earlier in Chapter 3 implied. The fouling tendency evaluation can be approached from many perspectives, including fuel-based in-

dices, chemical equilibrium calculations or computational fluid dynamics (CFD) modelling. Modern modelling techniques give a better chance to focus on determining the deposition mechanism besides estimating the actual rate of build-up. On the other hand, traditional fouling indices can be fine-tuned e.g. with chemical fractionation, which is used to separate the reactive and non-reactive compounds in the fuel. Therefore, it is hard to determine a single best method to evaluate the fouling tendency, but some examples of evaluation attempts are briefly reviewed here. Emphasis is given on biomass and waste fuel applicability of the presented evaluation methods because of their importance in fluidized bed combustion. [60, pp. 34–35]

3.5.1 Fouling indices

Indices based on elementary fuel composition can be regarded as the traditional way of fouling tendency prediction and they have been used for some decades for coal fuels. The idea of the indices is to compact the effect of various ash formation contributor elements into single figures that serve as indicators of the fouling tendency severity. According to Theis [60, p. 35] and Teixeira et al. [59, p. 193], perhaps the most common of these indices is the base-to-acid ratio. It is used to estimate the effect on ash fusion temperatures that the varying amount of basic oxides relative to acidic oxides has. The ratio is presented as

$$R_{B/A} = \frac{Fe_2O_3+CaO+MgO+K_2O+Na_2O}{SiO_2+TiO_2+Al_2O_3}, \quad (1)$$

where the oxides are given as mass fractions in the ash content. At least for coals, the base-to-acid ratio, or its simplified form that excludes TiO_2 and alkali oxides, is connected to ash melting temperature reductions in a parabolic relation. According to the literature review by Pronobis [49, p. 377], the worst slagging occurred with the ratio number 0.75. Below 0.15 the hemispherical temperature is considered to be high enough to cause no risk and for $R_{B/A} \geq 2.0$ the correlation between the oxide concentrations and the ash HT and FT temperatures is no longer clear. This reduces the applicability of $R_{B/A}$ index for fouling prediction of high-alkali biomass fuels such as straw, as the ratio can easily exceed 2.0 because of the high basic element content in the fuel feed. The simplified form of the ratio serves biomass fouling tendency evaluation purposes even more poorly, as the alkali elements are excluded completely in it. [59, p. 193]

A common index used for slagging estimation is the ash content based $R_{B/A}$ coupled with S content in the dry fuel substance, presented as

$$R_s = R_{B/A} S_{d.s.}, \quad (2)$$

and it also has limited usability for biomass fuels, as they tend to have relatively low sulfur content. However, it may be helpful when evaluating the overall effect of co-combustion fuel mixtures consisting of coal and biomass. Slagging risk is considered to be low for R_s values under 0.6 and on the other end extremely high for $R_s \geq 2.6$. Looking only at this indicator, it could seem that the alkalis from the biomass and the sulfur from coal would be an inevitably problematic combination, but one should bear in mind that the relatively low furnace temperatures in FB boilers reduce the risk of ash melting in comparison with PC boilers. [49, p. 377]

A fouling index similar to the slagging estimation R_s is presented in Equation (3). It highlights the importance of alkali oxides in the fouling phenomenon. However, the neglect of chlorine and sulfur is a drawback in terms of the usability of this index, because their impact on behavior of the alkalis can be drastic. In Pronobis's review [49, p. 377] the index is defined as

$$F_u = R_{B/A} * (Na_2O + K_2O), \tag{3}$$

where the Na and K oxides are given as mass fractions in the ash, as in the $R_{B/A}$ ratio in Equation (1). A similar ratio is given by Raiko et al. [50, p. 295] but K_2O is excluded from it. In the form of Equation (3), it is claimed that $F_u \leq 0.6$ implies a low tendency for fouling and $F_u \geq 40$ means an extreme risk for deposit build-up and sintering.

Majority of fouling-related ash research focuses on alkali metal, Cl and S compounds, but the effect of phosphorus is widely neglected, as the exclusion of phosphoric oxides from the indices in Equations (1-3) indicates. Agricultural fuels can contain substantial amount of phosphoric compounds: for example, average P concentration in the ECN database [16] is 28 g/kg in d.s. for sewage sludges, 29 g/kg in d.s. for meat and bone meal and 21 mg/kg in d.s. for chicken manure. For comparison, the mean P content for both, the wood chips selected to Table 2 and also for coals of varying ranks is only 0,4 g/kg in d.s. Phosphorus may induce ash sintering via formation of alkali phosphates and in order to address this possibility, Sommersacher et al. [55] presented a new index, given as

$$R_P = \frac{Si+P+K}{Ca+Mg}, \tag{4}$$

where all elementary values are given in moles, and so form a molar ratio. Increasing R_p ratio correlates with decreasing ash sintering temperature and thus an increasing tendency for slagging and fouling issues. [48, p. 61], [55, pp. 388–389]

All the indices presented above assume that the amounts of the compounds in ash for Equations (1-4) have an integral role in the ash melting behavior and therefore affect fouling tendency heavily. While this is generally accepted, Teixeira et al. [59, p. 193] emphasize the fact that these indices do not take the reactivity of the related elements in the fuel into account. The indices themselves might give rather reliable estimations of the

fouling tendency, but the oxide mass fractions that are used in them could perhaps be seriously incorrect if the reactive and non-reactive shares of each element in the fuel are not decently separated.

The ash fusion temperatures that were discussed in Paragraph 3.2.2 are determined in an atmosphere consisting of either air or a mixture of CO and CO2, which are called oxidizing and reducing conditions respectively. If the ash fusion temperatures are determined according to the ASTM or DIN standards, the results can be used for fouling prediction. As the purpose of the indices in Equations (1-3) is to estimate slagging or fouling via the ash melting behavior, the direct ash fusion temperature index might correspond to the fouling phenomenon more accurately. The ash fusibility index (*AFI*) is given as

$$AFI = \frac{4*IDT+HT}{5}, \tag{5}$$

where IDT is the initial deformation temperature and HT is hemispherical temperature. This index can give information of the fouling tendency even though the F_u index in Equation (3) would be incorrect. For example, in Dunnu's et al. [14] study for SRF fuel ash characteristics and deposition, *AFI* was in good accordance with other indices and SiO_2-CaO-Al_2O_3 equilibrium phase diagram, but F_u did not match with them properly. Teixeira's et al. experimental results also matched the evaluated *AFI*-based predictions to a certain extent. Calculated from their ash fusion temperature results, *AFI* value was 888 °C for straw pellet sample and 1228 °C for Polish coal sample. These values make sense in regard to the known problematic nature of straw and easiness of coal, since the lower the value is, the higher fouling risk it implies. [14, p. 1539], [59, pp. 194–202]

The accuracy of all indices described above, including *AFI*, is limited by disregard of atmosphere characteristics. For example, the ash fusion temperatures measured in laboratory conditions may differ from the actual ash phase change temperatures in real combustion. Temperature gradients, flue gas velocity and particle impaction phenomena among other factors make estimation of real fouling harder. The indices can give some rough predictions, but the review by Garcia-Maraver et al. [25, p. 10] revealed that there is not any fully reliable agreement even between the common indices, including the ones presented in Equations (1-3) and (5).

Another drawback of the traditional indices in Equations (1-3) is that they were originally developed for coal fuels. Fluidized bed combustion applications call for refined fouling indices for biomass and waste fuels, which require a new approach to weighing the effect of each significant element in the indices. Sommersacher's et al. [55] study on phosphorus is an example of this. Teixeira et al. [59] only mentioned the ash fusibility index of Equation (5) to be applicable for the biomass fuels the studied, but even the fusibility approach can be faulty, because the standard measuring method of the fusion temperatures might leave droplets of molten phases unnoticed. Thus, further research on indices focusing on usability with biomass is needed.

3.5.2 Thermodynamic equilibrium models

Modelling of chemical or thermodynamic equilibrium is another approach to evaluate slagging and fouling tendencies of solid fuels. When combined with extensive fuel analyses - e.g. analyses that include chemical fractionation - and some key operating parameters, equilibrium modelling can give moderately accurate implications of the fouling process. Moradian et al. [41] applied a thermodynamic equilibrium model for fouling evaluation of a BFB boiler combusting solid waste. In addition to advanced fuel analyses, they utilized measured temperature distribution, pressure and air-fuel ratio data in the evaluation. As limitations for the thermodynamic equilibrium modelling accuracy, Moradian et al. mention the imperfection of available thermodynamic databases, focus on chemical properties leading to exclusion of physical attributes and the assumption of all reacting particles reaching equilibrium in the process. [41]

The operational principle of Moradian's et al. three stage calculation tool is shown in Figure 10. It utilizes FACT thermodynamic database data with Gibbs energy minimization technique. Thermodynamic equilibrium for each calculation stage was considered for 16 elements deemed as most reactive and significant, ending up with an evaluation of the chemical atmosphere on superheater tube surfaces. The three stages in Figure 10 were chosen to appropriately represent the distinctive zones of a BFB furnace.

A stage division somewhat similar to that of Figure 10 was presented also by Nutalapati et al. [44], who named the stages as radiative section and high and low temperature fouling sections, based on temperature regimes. Their study was not performed on fluidized bed boiler specifically, though. Comparison with actual deposit characteristic measurements conducted on deposit probes by Moradian et al. showed a correspondence with the calculated thermodynamic model results, but also some considerable differences for some test cases.

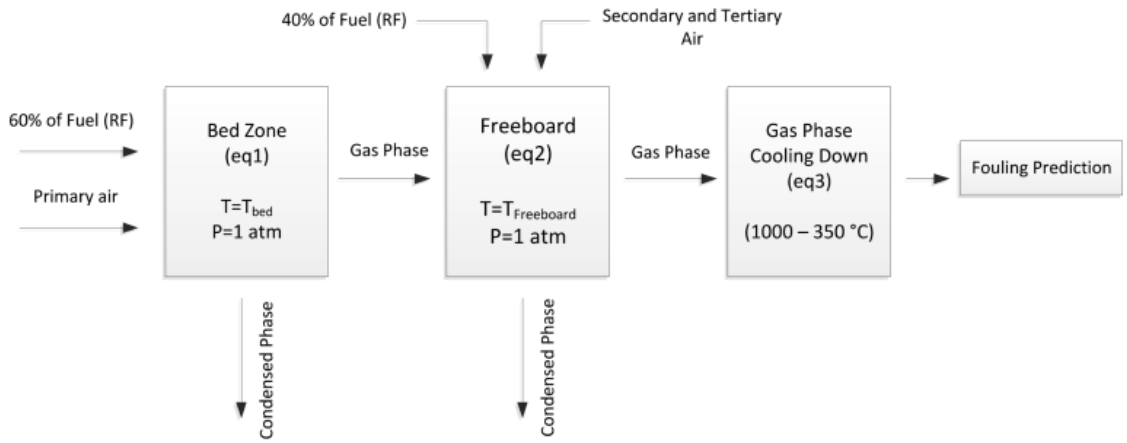

Figure 10. *Equilibrium modelling stages in Moradian's et al. study* [41, p. 3486]

The modelled fuel in Nutalapati's et al. [44] evaluation was wheat straw, producing rather expected results that implicate high releases of potassium compounds. Gaseous KCl was

estimated to be the most thermodynamically stable potassium compound in all of the three evaluated temperature regimes (500-900 °C, 900-1300 °C and 1300-1600 °C), with formation of gaseous KOH and potassium silicates and sulfates depending on the amount of available Cl to react with K. Nutalapati et al. used chemical fractionation and performed evaluations with two models; first one that only utilized reactive fractions (water and acetate leachable parts) of the fuel, and second one that also considered some portion of HCl solubles and residue fractions to be reactive, despite the assumption of low non-reactive potassium content given originally by Miles et al. [39, p. 131].

Conclusion from the results of the two models was that because of molten phase content differences, the first model acknowledged high fouling and moderate slagging and the second model estimated less severe fouling but worse slagging effect, highlighting the importance of correct assessment of chemical fractionation. The models were not validated with experimental results though, so performance comparisons are somewhat theoretical. [44, p. 1052]

Factsage, the database program that was used by Moradian et al. [41], was also the equilibrium calculation data basis for Stam et al. [57], who compared thermodynamic fouling predictions to actual deposit samples in a BFB boiler. Furthermore, Stam et al. also used chemical fractionation data to differentiate between reactive and non-reactive constituents in the fuel, but like in Nutalapati's et al. study, some of the elements thought to be non-reactive were considered in the evaluation too. In their study, the fuel mixture was wood-based. Deposition rate differences for two rather similar fuel blends were matching between the calculations and measured deposition probe results, implying a sound performance of the model. As a perhaps more significant conclusion however, Stam et al. presented that the evaluation of amount of molten salts, which in turn depicts the maturity and build-up potential of the deposit, should be based on the equilibrium calculations at the deposit temperature instead of conclusions drawn from total ash content and expected shares of salts in it. [57, p. 330]

3.5.3 Fouling tendency evaluations based on CFD modelling

As the operational factors of the boiler have a notable effect on the fouling tendency alongside the combusted fuel matter, computational fluid dynamics (CFD) has been used to try to model the combustion process and atmosphere in the furnace and convective parts of various boiler types with a special emphasis on deposition phenomenon. However, a literature review by Weber et al. [64, p. 120] points out that these surveys are not numerous, and even fewer have been specified to fluidized bed boilers. There is also variation in included input parameters: for example, some models in Weber's et al. review use only inertial impaction to evaluate ash particle transport to the tube surface, while others take Eddy diffusion and thermophoresis into account too. Ash stickiness is generally evaluated in these CFD models by viscosity sub-models or melting behavior curves.

In this respect, the fouling indices and results from thermodynamic equilibrium models can serve as valuable input feed calculations for the CFD models.

Mueller et al. [42] examined CFD modelling of wood combustion in a BFB boiler. Even though they only included inertial impaction for ash transport evaluation, the model estimated the location of severe slagging in the furnace correctly. The inclusion of boiler geometry is indeed a major advantage of CFD modelling of ash deposition. Mueller's et al. study took advantage of chemical fractionation to give precise input for the model. Thus, it is possible to benefit from combining different slagging and fouling tendency estimation methods: in Mueller's et al. study the modelling provided the location of occurrence, enabled by using other indicators (chemical fractionation results) to verify the possibility of the slagging phenomenon in the first place. In other words, there is no single method that alone could give proper information of the location, formation, phase and build-up rate of the deposition – or if the overall CFD modelling procedure is considered as a single method, it is rather time-consuming anyway.

Ash deposition in co-combustion of coal and various biomass fuels has been recently modelled with CFD by Garba et al. [24], Yang et al. [66] and Taha et al. [58], for example. Garba et al. used CFD modelling to estimate slagging propensities of various coal-biomass mixtures in an entrained flow reactor. As was the case in Mueller's et al. study, the model performed qualitative prediction of deposition reasonably well. A slagging index was calculated with the model and used to rank the biomass fuels by deposition efficiency, indicating more severe slagging for olive and palm than for miscanthus, for example. This finding matched the experiences from actual combustion at the modelled flow reactor, but the quantitative deposition results were somewhat lacking [24, pp. 870–871].

Entrained flow reactor was also observed by Yang et al., who studied palm kernel co-combustion with coal. They found an acceptable agreement between experimental and modelled deposition efficiencies, implying increasing deposition occurring by increasing share of palm kernel in the fuel mixture, but as a downside of the model, the sensitivities to impaction characteristics and particle stickiness variation were acknowledged as well [66, pp. 47–48]. Increasing share of biomass leading to higher risk of slagging in the evaluated tangentially fired boiler was found also by Taha et al. They discovered that the high volatile content of meat and bone meal could shift the slagging forward in the convective heat exchanger part of the boiler, away from the furnace, by increasing flame heights [58, p. 134].

According to the existing CFD models, it is feasible in some cases to use modelling to locate areas in furnaces that have increased risk of deposition. In addition, expertise and decent fuel analyses at the very least are required to estimate more specific slagging and fouling characteristics on the deposition locations. The main objective of the experimental

part of this thesis is to find relations between the deposition build-up and various operational parameters, to evaluate the fouling phenomenon in full scale boilers without the use of time-consuming CFD modelling.

3.5.4 Deposit build-up evaluation by weight measurements

Another approach to evaluate the degree of fouling is determining the actual amount of the mass that the forming deposit adds to the heat exchanger elements. Namkung et al. [43] used a real-time measurement system that is based on an electrical balance measuring the weight of ash that accumulates on a collector plate. Their study was conducted in a lab-scale drop tube furnace operating in gasifying conditions and this exact kind of experimental test system could perhaps not work in a large-scale grate, PC or FB boiler.

Despite Namkung's et al. test system does not apply well for fluidized bed boiler applications, a clear, general relation between the changes in chemical composition of the gasified coal samples and the measured deposit build-up could be deduced from the results. Namkung et al. assumed that the role of Fe and Ca would be significant in the deposit build-up process, and the scanning electron microscopy (SEM) analyses performed on the measured deposits showed that increasing share of Fe and Ca compounds in the ash indeed had an increasing effect on the ash accumulation on the weight measurement plate. This finding is depicted in Figure 11, which shows a clear slowing change of the deposit build-up rate at the 30-minute mark – and the SEM analysis results indicated a clear decrease in the Fe and Ca content of the deposit from that point onwards. [43, pp. 213–217]

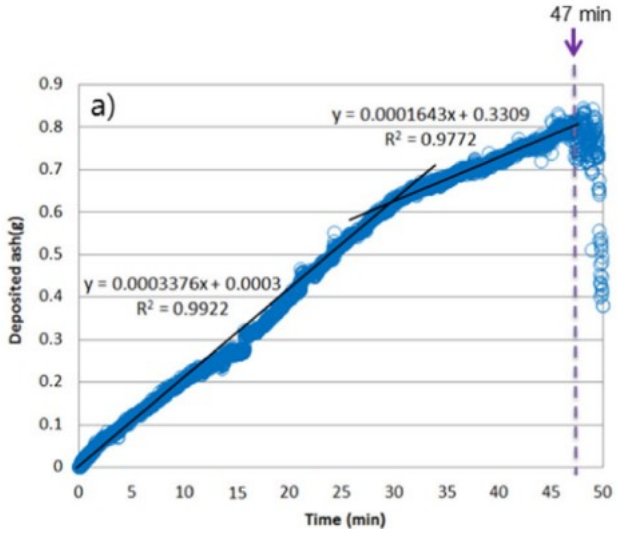

Figure 11. *Deposit build-up rate in Namkung's et al. study* [43, p. 213]

A commercial weight measurement based soot blowing optimization system has been developed by Endat, part of Clyde Bergemann Power Group. Their basic concept of evaluating the fouling by deposit weight gain is the same than that presented by Namkung et al. [43], but the implemented measurement solution represents a different approach,

which is intended for on-line measurement purposes in large boilers. The measurement is based on SMART Gauge Sensor, a strain gauge that measures the increasing weight of the heat exchanger elements from their hanger rods. As the deposit builds up, the strain on the hanger rods grows and this measurement can be changed into localized weight gain information for the superheaters, economizers or any heat exchangers that are supported by rigid rods from above. However, it should be noted that the fouling examination technique based on weight measurements is not predictive by nature, like the fuel-focusing fouling indices, thermodynamic equilibrium calculations or CFD models are. [11], [30]

3.5.5 Heat transfer based validation

The methods utilizing heat transfer calculations in fouling phenomenon validations are all – by fundamental idea at least – based on the thermal resistance of the deposition layer emerging on the heat exchanger tube surfaces. Common methods of calculating basic heat transfer balances in parallel, counter or cross flow heat exchangers include effectiveness and number of transfer units (NTU) and logarithmic mean temperature difference (LMTD) approaches [40, p. 669]. The basic idea of the NTU method is to form heat capacity flows from the mass flows entering the heat exchanger, and then dictate the maximum heat $\dot{Q}_{max}$ by the smaller of the heat capacity flows (C_{min}) and inlet temperatures ($T_{H,in}$) and ($T_{C,in}$) and use these to calculate an unknown outlet temperature. An effectiveness factor can be formulated by comparing the heat flow in either the hot or the cold side to the maximum heat:

$$\varepsilon = \frac{\dot{Q}}{\dot{Q}_{max}} = \frac{C_H(T_{H,in}-T_{H,out})}{C_{min}(T_{H,in}-T_{C,in})} = \frac{C_C(T_{C,out}-T_{C,in})}{C_{in}(T_{H,in}-T_{C,in})}, \quad (6)$$

where $\dot{Q}$ represents the actual heat transfer as the enthalpy change in either the hot (or cold side. C and T stand for the heat capacity flow and temperatures on the subscripted side of the heat exchanger, respectively. The effectiveness factor (ε) is then combined with the number of transfer units (N_{tu}) and capacity ratio (R_c). N_{tu} is defined as

$$N_{tu} = \frac{UA}{C_{min}}, \quad (7)$$

where U is the overall heat transfer coefficient and A is the total outer surface area of the heat exchanger tubes. The capacity ratio (R_c) is

$$R_c = \frac{C_{min}}{C_{max}}, \quad (8)$$

where C_{max} is the larger of the heat capacity flows, contrary to C_{min} described earlier. These ratios and factors can be joint in various Equations, depending on the heat exchanger configuration. Effectiveness factor can be calculated out of those Equations and then one unknown outlet temperature can be figured out by using Equation (6). In parallel-flow heat exchanger for example, the relation between ε and N_{tu} would be of form

$$\varepsilon = \frac{1-e^{-Ntu(1+R_c)}}{1+R_c}. \quad (9)$$

Basic formulation of the LMTD method might seem more straightforward, but requires known values of all inlet and outlet temperatures. A general heat transfer formulation by the LMTD is

$$\dot{Q} = UA\Delta T_{lm} = \dot{m}_{cold} c_{p,cold} (T_{out} - T_{in})_{cold}, \quad (10)$$

where U and A represent the overall heat transfer coefficient and total outer surface area of the heat exchanger, as in Equation (7), $\dot{m}_{cold}$ is the mass flow of the cold side of the heat exchanger and $c_{p,cold}$ is the specific heat capacity at the average value of the cold stream temperatures T_{out} and T_{in}. The logarithmic mean temperature difference (ΔT_{lm}) can further be defined as

$$\Delta T_{lm} = \frac{\Delta T_0 - \Delta T_1}{\ln(\frac{\Delta T_0}{\Delta T_1})} = \frac{(T_{H,in} - T_{C,out}) - (T_{H,out} - T_{C,in})}{\ln(\frac{(T_{H,in} - T_{C,out})}{(T_{H,out} - T_{C,in})})}, \quad (11)$$

where the temperature subscripts follow the same logic as in Equation (6). The calculation of ΔT_{lm} depends on heat exchanger configuration, and the form of Equation (11) is for counter flow exchanger. Temperature changes along flue gas duct of a counter flow superheater can be seen in Figure 12, where the ΔT_0 and ΔT_1 markings from Equation (11) are illustrated too. In other words, the x-axis in the figure represents pathway of the flue gas in the direction of its flow.

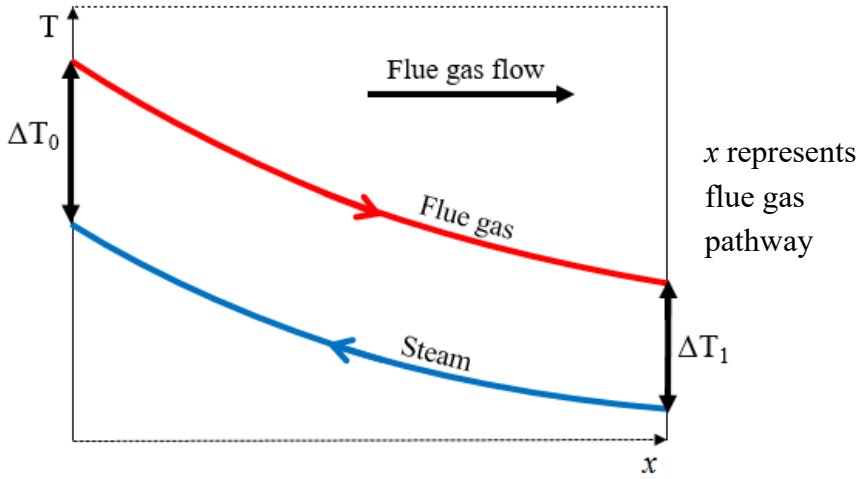

Figure 12 *Temperature changes in a counter flow superheater*

The U value can be calculated using Equation (10), if the mass flow on the cold side and all the inlet and outlet temperatures are known, and then compared with reference heat transfer coefficient to evaluate how a deposit has altered the heat transfer from the flue gas to the air, water or steam stream. This way a thermal resistance (r) of the deposit layer can be formulated from the coefficient comparison:

$$r = \frac{1}{U_{fouled}} - \frac{1}{U_{clean}}, \tag{12}$$

where U_{clean} is the reference heat transfer coefficient and U_{fouled} is the calculated coefficient of the fouled heat exchanger. [40, pp. 669–671], [45, p. 1240], [53, p. 946]

Oh et al. [45] used the LMTD method to evaluate fouling issues of cattle biomass combustion in a small-scale downward-fired boiler. They found out that in this specific small-scale boiler, the initial deposition on the low temperature heat exchangers improved heat transfer momentarily, assumedly due to change in radiative heat transfer. Further deposit build-up resulted in perhaps a more intuitive, weakening effect on the overall heat transfer coefficient and so generally the U value decreased by increasing deposit accumulation on the tubes. The calculation approach focusing on comparisons of overall heat transfer coefficients was also used by Mann et al. [38], for example. They used the calculations to evaluate the performance of different soot blowing technologies, and over an extensive measurement period it was concluded that sonic sootblower worked better than a steam sootblower, and they both outperformed a tested explosion soot cleaning system [38, p. 30].

Abd-Elhady et al. [2] included another heat-transfer-focusing evaluation in their study of deposit sintering on the surface. They also simplified the calculation by observing changes only in the overall heat transfer coefficient from the hot to the cold flow, without a focus on the thermal resistance of the deposit layer specifically. The same rising trend of increasing thermal resistance because of fouling can be seen in their results. In the above-mentioned studies, a fluidized bed boiler was the type of the reviewed boiler only in Mann's et al. study, but the relevant fouling calculation mechanisms are assumed to be rather independent of the boiler technology.

One significant limitation on all the fouling validation mechanisms based on either weight measurements or heat transfer weakening is the general assumption that the solid deposit that sticks to the tube is the sole variable in the mass of the tube element or in the heat transfer from the flue gas to the heat receiving agent. Corrosion, which is a typical consequence of fouling, can diminish the mass of the tube metal and thus cause error to the weight measurement and simultaneously alter the heat transfer characteristics of the clean reference state of the heat exchanger. This issue is particularly significant to keep in mind when performing evaluations on the in-house tool or when using the commercial weight measurement systems, as they are both targeted at validating the fouling phenomenon from a continuous operation period of the boiler, during which precise data of the condition of the tube material itself can hardly be received.

4. FOULING EXAMINATION UTILIZING MEASUREMENTS AND IN-HOUSE CALCULATION TOOL

The aim in the computational part of this thesis was to analyze actual fouling rates in real fluidized bed boilers, using measured automation data from each studied boiler. Fouling rates were calculated on an in-house program. This tool utilizes hot and cold side temperature and mass flow measurements separately for each heat exchanger to define experienced reduction on heat transfer caused by fouling over time. Five FB boilers were selected for comparison. The process data based evaluation inevitably excluded detailed chemical atmosphere at the tube surface from consideration. The purpose of this examination based on heat transfer was more to express a manifestation of actual fouling phenomenon in large scale boilers, rather than to try to give new insight on the fouling prediction, which was the main target of fuel-related approaches represented in Chapter 3.5 by the indices, thermodynamic equilibrium models and CFD modelling.

A general overview of the data handling process is depicted in Figure 13. The stages mentioned in the chart are explained more in detail in Chapter 4.2,but the conducted work could be divided roughly into preparation phase before calculations on the tool first, and secondly into analysis phases of the thermal resistances and fouling rates. Majority of the visible results originate from work package 8. in Figure 13, where the truly relevant analysis was done from processed data.

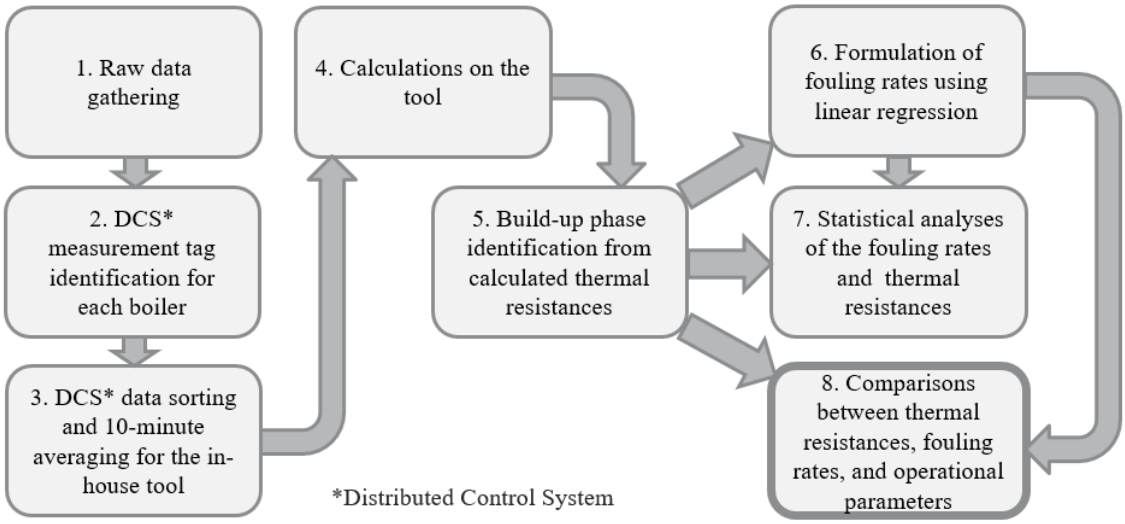

Figure 13 *Data handling procedure*

The in-house tool applies the basic LMTD method described in Chapter 3.5.5 with some refinements. Calculation can be performed on a superheater, economizer or air preheater.

As fixed input parameters, the program requires an approximated reference state for the flue gas mass flow and the modelled heat transfer coefficient at clean conditions, where no deposit exists on the tube surfaces, plus the total outer surface area of the examined tube elements.

The thermal resistance was calculated for each measured time stamp separately. The mass flows and temperatures were compared to heat exchange at reference state to evaluate the effect of forming deposit on the heat transfer. The program iterates the value of either mass flow or an inlet or outlet temperature in the heat exchanger until the resulting heat transfer balance converges, and simultaneously a thermal resistance value of the possibly formed deposit is calculated. The reference value for overall heat transfer coefficient is essential – otherwise the calculation would not have sufficient input information. On the other hand, one mass flow or temperature value must be left out from input data, even though the measurement values would be available, because otherwise the calculation case would be over-defined.

At the beginning of the work, the in-house tool was not fully ready to use yet. Testing, troubleshooting, and tweaking was done in co-operation with Pauli Haukka, programmer of the tool. While the case calculations were initiated soon after basic usability of the tool was reached, continuous fixing of usage-related bugs was kept going alongside the calculations. Some unexpected delay was experienced from changing the heat transfer calculation principle from NTU method to LMTD.

4.1 Determination of process-based fouling indicators

One of the set research questions was to identify main operational parameters that affect fouling. The most prominent measurable factor in changes of thermal resistance of the deposit layer is probably soot blowing. Periodic operation of the soot blower helps in keeping the tubes relatively free of deposits – although the ability to clean the tubes by soot blowing depends heavily on the sticking properties of the formed ash. Periods of soot blowing seem to be a dominant cause of temporarily improved heat transfer in Peña's et al. [47, p. 740] calculation results, but drops in thermal resistance of the deposit layer are still numerous outside soot blowing periods too. As discussed in Chapter 3.4, deposits can fall off the surfaces by erosion, gravity shedding and thermal or mechanic tension changes, all besides the forced soot blowing pulses. This variety makes estimation of the root cause behind each momentary drop in thermal resistances challenging, in case the drop would not match with a soot blowing period. However, greater research interest in the fouling examination in this thesis is directed at the deposit build-up phase anyway, not the shedding phenomenon.

The chemical composition dependency of the ash stickiness and consolidation on the tube, described in Chapter 3, implies that the combusted fuel mixture is an integral factor of the deposit build-up. The selected test cases consist of specific test points, during which

a pre-determined fuel feed mixtures were held constant for several hours. One target of the fouling validation here is to be able to identify these test points in the calculated thermal resistance fluctuations.

Other factors originally selected for comparative examination were velocity of the flue gas – projected against varying tube pitches of the heat exchangers – and fuel load changes. It has been estimated that lower flue gas velocities reduce fouling rates due to reduction of depositing material facing the tubes [69, p. 1532]. Effect of particle velocity on sticking propensity in waste incinerators was studied by Abd-Elhady et al. too [1]. Despite the velocity study would have been interesting, claimed inaccuracies in the flue gas flow measurements forced to move the examination focus from actual velocities to flue gas pressure changes along the studied heat exchangers. Although the simple Bernoulli's principle does not apply for compressible flue gases absolutely, the change in pressure difference was considered to represent the same phenomenon with the flue gas velocity fluctuation to an acceptable extent. In fact, Eklund and Rodin emphasized the effect of pressure change particularly, not the flue gas velocity [15, p. 79].

Catching the effect of boiler load change on fouling was expected to be challenging in the case of inclining deposit formation if the load change is insignificant, because it might be hard to determine between deposition dominance by challenging fuel composition and by subtly changing boiler load. Even so, Peña et al. gave a conclusion that fouling is much more severe under high load conditions than under lower load [47, p. 741]. As with the flue gas velocity examination, the known unreliability of on-line fuel load measurement led to a change of initial idea of utilizing direct fuel load figures, and so eventually calculated main steam power was studied instead. Fouling-wise, changes of the fired fuel load could be perhaps more prominent than those of the main steam, but the steam power fluctuation was expected to show similar correlation with fouling changes nevertheless.

4.2 Data collection for calculations and result processing

Four different CFB boilers and one BFB boiler were chosen to the calculation case matrix. These boilers use distinct fuel mixtures and vary also structurally, which together mean also diverse experiences of fouling issues in them. The boilers were selected based on specific and documented combustibility campaigns, guarantee test or probe test periods that had taken place in them. This was done to be able to link the calculation results to detailed fuel mixture information that would not be accessible afterwards from regular operation periods, when only basic systematic analyses are conducted on the fuel at the most.

The measurement data was retrieved from the distributed control system (DCS) log files and processed to fit the in-house calculation tool. Alongside the required flows and temperatures, other operational parameters were also collected from the raw data, including calculated fuel loads, soot blowing steam flows, and pressure changes on the flue gas side

of the ducts. A summary of the measurements can be found in Table 6. Original data had one minute measurement intervals in each boiler, but since the timespan of the calculation cases extended over several days, a 10-minute interval was concluded to be sufficiently representative. In addition, the longer intervals had lower required computation time as well, and so the one minute data was averaged into 10-minute intervals before calculation (work package 3. in Figure 13).

Table 6 *Selected DCS and process modelling data for the calculations*

Measured variables and constants	Raw unit in DCS or modelling	Source
Flue gas temperatures in and out (for each heat exchanger)	°C	DCS
Steam or feedwater temperatures in and out (for each heat exchanger)	°C	DCS
Steam or feedwater mass flow (for each heat exchanger)	t/h or kg/s	DCS
Soot blowing steam flow	t/h or kg/s	DCS
Pressure drops in flue gas side	Pa or mbar	DCS
Main steam parameters	°C, bar and kg/s	DCS
Heat exchange surface area	m^2	Boiler design data
Heat exchanger tube and element pitches	mm	Boiler design data
Reference value for overall heat transfer coefficient	W/m^2K	Boiler design data

Mass flow of steam was measured only after all superheaters by default, e.g. from the main steam tube before the turbine. Water spray flows added to this main steam in attemperators after primary and secondary superheaters were acknowledged by subtracting them respectively from the main steam mass flow values. In most cases, the feedwater flow measurement before economizer took place before the separation of water to the attemperators, so the total flows to attemperators had to be subtracted from the feedwater flow measurement as well to give precise input for the fouling calculations of economizers.

Geometrical data, including tube and element pitches, and the reference heat transfer coefficients for each heat exchanger element were gathered from the designed process modelling data of each boiler. The elementary composition of the flue gas, that was utilized in the molar mass calculations for determining the specific heat capacities of the flue gas, was also fetched from the process modelling results, since it was thought to be a sufficiently constant parameter in each boiler's case individually, despite how the fired fuel feed changes the composition slightly.

Air preheaters were left out of examination because of assumed significant inaccuracy related to overly high equivalence of temperature values on the hot and cold, or flue gas and clean air sides of air preheaters. For the evaluated superheaters and economizers, the measurement of steam temperatures were assumed to be more precise than possibly varying temperatures of flue gas, but the measurement of the volumetric flue gas flow was considered to be even more uncertain than that of the temperatures. Therefore, the flue gas flow was set as the variable to be calculated in the in-house program. The evaluated test matrix is shown in Table 7, where the abbreviations SSH, ECO and PSH refer to secondary superheater, economizer and primary superheater respectively.

Table 7 *Test matrix of the fouling examinations*

Boiler case number	Boiler type	Examined heat exchangers
1	CFB	SSH, ECO
2	CFB	SSH, ECO
3	CFB	SSH, ECO
4	CFB	PSH, ECO
5	BFB	PSH

Despite the similarity of the evaluated superheaters appears to be a bit low in Table 7, it should be noted that since the phenomenon to be validated is the outer surface fouling of the tube elements, the flue gas side temperature range at the given heat exchangers is of higher interest than the actual superheating stage of the steam. The studied boilers have varying superheater and economizer configurations, meaning that a universal definition of the flue gas temperature range by each superheating or feedwater heating stage cannot be made. A refined categorization based on distinct temperature ranges is presented in the results section.

Research targets included estimating the applicability of the heat transfer method and the correlation strength with selected operational parameters, and so basic statistical correlation analyses were conducted. Uncertainty could have been caused by various issues. Continuous flue gas temperature measurement is a good example of the calculation tool input values that have high susceptibility for measurement error. As the thermoelements are typically rather near the duct walls, the temperature difference between the measurement point and the centerline of the flue gas flow facing a superheater or economizer can be even 100 °C. Varying flow patterns make implementation of a constant correction factor to this unavoidable error challenging. Partly due to these measurement errors, rather low attention was paid on the raw and discrete calculation values themselves. Instead,

time-dependency and the rate of the calculated thermal resistance values by each test point of the combustion campaigns were studied further.

Time series analysis on the calculated values was done by line fitting with linear regression to catch the rate of thermal resistance build-up. Pearson's coefficient of determination was also calculated to evaluate the differences in the calculated fouling rates; some cases were found to express almost asymptotic behavior in thermal resistance build-up, whereas others showed steadily rising resistance values until the following soot blowing pulse. Microsoft Excel was used in the linear regression and Pearson product moment correlation coefficient (*PPMCC*) calculations, using LINEST and RSQ functions. It should be noted that while *PPMCC* is a measure of the applicability of the linear trendline formed over specific data points, it cannot analyze properly the nature of the deviation from a perfect line. In other words, a similar *PPMCC* value can be formed for a data set with considerable deviation between adjacent data points but strongly linear overall trend, and for a clearly non-linear set with minimal deviation.

Several comparisons using calculated thermal resistances were conducted in the computational part. One of these was comparison against fired fuel mixture. To gain comparable data for the fuel mixture examinations, the effect of boiler load change was formulated into alternative fouling rate figures, mainly because of one considerable load change in boiler 1. The steam power adjustment was performed for the boiler cases by dividing thermal resistances by the ratio of corresponding steam flow measurements to average steam flow, as per equation

$$r_{s.a.} = \frac{r}{\left(\frac{P_{steam}}{P_{steam,avg}}\right)}, \tag{13}$$

where r expresses an original thermal resistance value, P_{steam} is the calculated steam power value at the timestamp of r, $P_{steam,avg}$ means average steam power from the whole campaign period and $r_{s.a.}$ is the resulting steam power adjusted r value. Effect of this equation is discussed in Chapter 5.5.

5. RESULTS AND DISCUSSION

Several different comparisons can be drawn from the calculation data. General examination of thermal resistances, time-matching of resistance surges with soot blowing operation and correlations with steam power change, flue gas pressure change and varying fuel mixture are presented individually for best representative calculation cases. Comparisons between boiler cases and boiler types are also presented, but they should be viewed with greater caution, as the possibly varying measurement accuracies might have been carried into variations of the resulted thermal resistances respectively. In other words, results from some boilers might be fundamentally more accurate than others. However, the fairly consistent overall value range of the fouling rates implicates that the deposition at least affects the overall heat transfer rather universally. Suggested differentiating factors are considered in discussion section in Chapter 5.8.

5.1 General appearance of thermal resistance calculations

The most fundamental research question was: "*Is heat transfer examination an applicable method to examine fouling of heat exchangers in fluidized bed boilers*"? To determine the answer to this, the nature of the calculation results was studied. Increasing deposit mass on the heat exchanger surfaces was expected to show a steadily rising trend in thermal resistance, as it was unanimously concluded in the studies reviewed in Chapter 3.5.5 [2], [38], [45]. Boiler case 1 was selected to demonstrate the related finding within this research. Figure 14 shows the relative thermal resistance (on a scale of 0-1) results of a five-day period for secondary superheater. The graph indicates a clearly – although not linearly – rising trend continuing until a swift plunge before each next build-up phase.

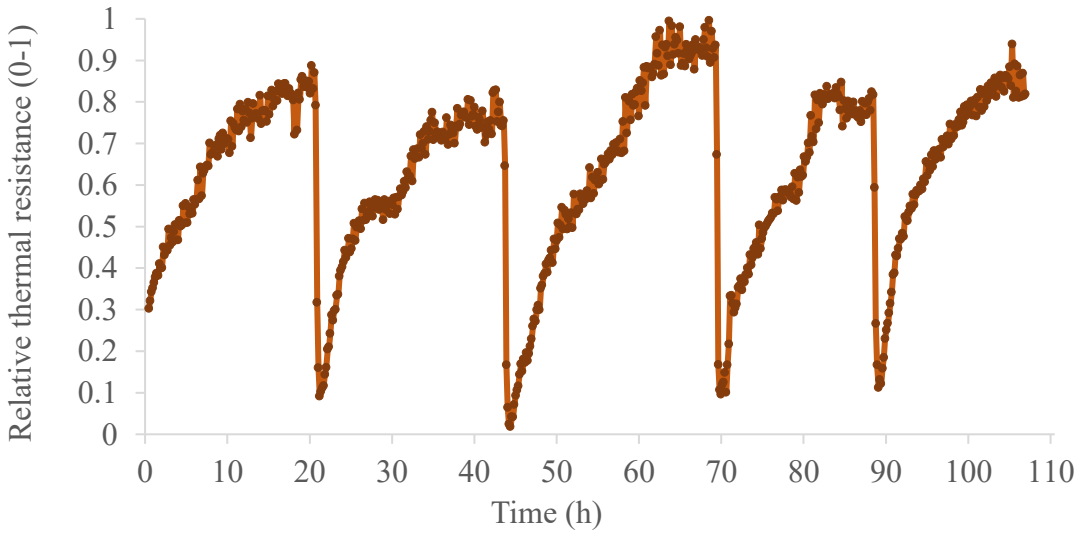

Figure 14. *Thermal resistance over a five-day period in boiler case 1, hot zone*

Before it can be concluded that the heat transfer calculations express fouling as clearly as Figure 14 implies, other factors causing the rising trends should be considered. As Equations (10-11) stated, a simple LMTD calculation requires knowledge of the mass flow on either side of the heat exchanger, inlet and outlet temperatures for both sides and the overall surface area to find out the *U* value used for reference state comparison. Tube area is considered to remain constant during the evaluation period, and hence only the steam mass flow and the four temperature measurements are the actual variables changing at each calculation point. These five measured attributes for the exact period of Figure 14 are shown in Figure 15.

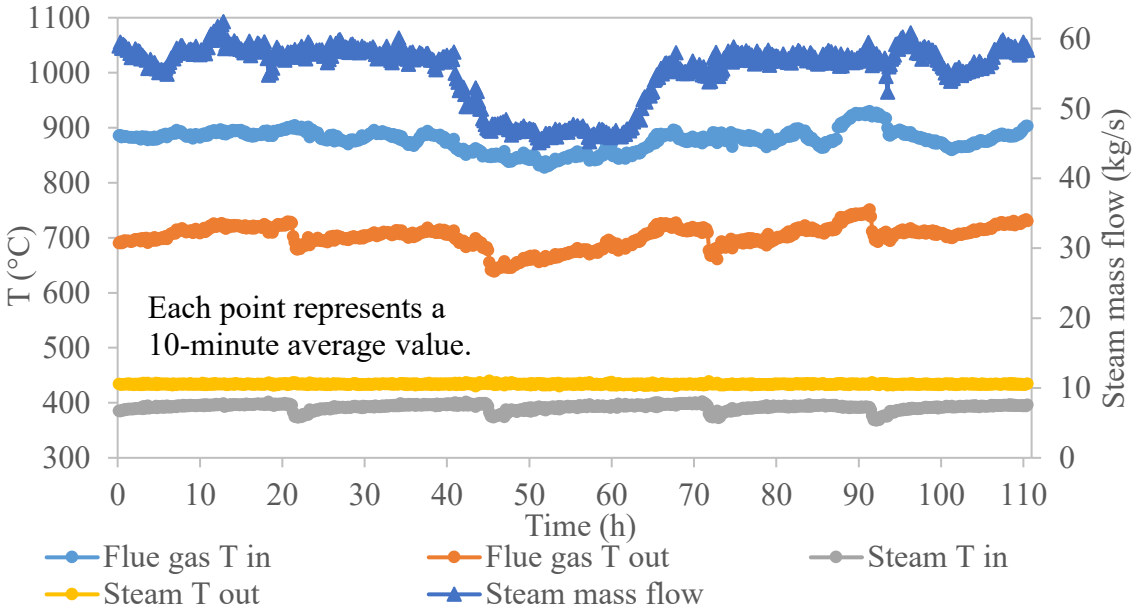

Figure 15. *Operational parameters from the calculation of boiler case 1, hot zone*

Parameter presentation in Figure 15 shows some key issues regarding the performance of the studied heat exchanger. The presented secondary superheater of boiler 1 is the first heat exchanger in the convective pass, e.g. the first tube element after the cyclone. Flue gas outlet temperatures (orange line) and steam inlet temperatures (gray line) appear to rise slightly and then drop in good accordance with thermal resistance values in Figure 14. The flue gas inlet temperature (light blue line) on the other hand seems to fluctuate inconsistently, while the steam outlet temperature (yellow line) draws a remarkably straight line.

When put together, these findings indicate that despite the steam outlet temperature is steady, the temperature difference between inlet and outlet of the steam side decreases periodically. Coupled with the increasing flue gas outlet temperature and steam mass flow that does not show clear trends, the decreasing steam temperature differences mark a worsening in the heat exchanger operation. In other words, less heat is transferred out of the flue gas into the steam, if the steam flow can be stated to retain its level. The sudden drop in the steam mass flow (blue line), visible in the middle of Figure 15, inevitably

affects this assumption by participating in the heat exchanger performance change, but not enough to prevent the temperature change pattern from being still visible in the graph. In conclusion, fluctuations seen in Figure 15 are essential for the result curves of thermal resistances, because the small temperature changes are the root causes of the rising trends of the resistances.

5.2 Effect of soot blowing in thermal resistances

Basic pattern of thermal resistances (r) of the deposits was shown in Figure 14 for an excerpt from boiler 1. Still it was not showed that it is absolutely deposition that causes the changes in temperatures, heat exchanger performance and calculated thermal resistances. The most evident indicator of deposit formation being the root cause of the changes is arguably the effect of soot blowing; if Figure 14 was a depiction of actual fouling, the cleaning effect of steam soot blowing pulses should match with the acute surges in r values. Figure 16 shows the situation for boiler 1 and the result is obvious: soot blowing indeed appears to cause the plunge in r value directly. The same effect occurred for all studied cases.

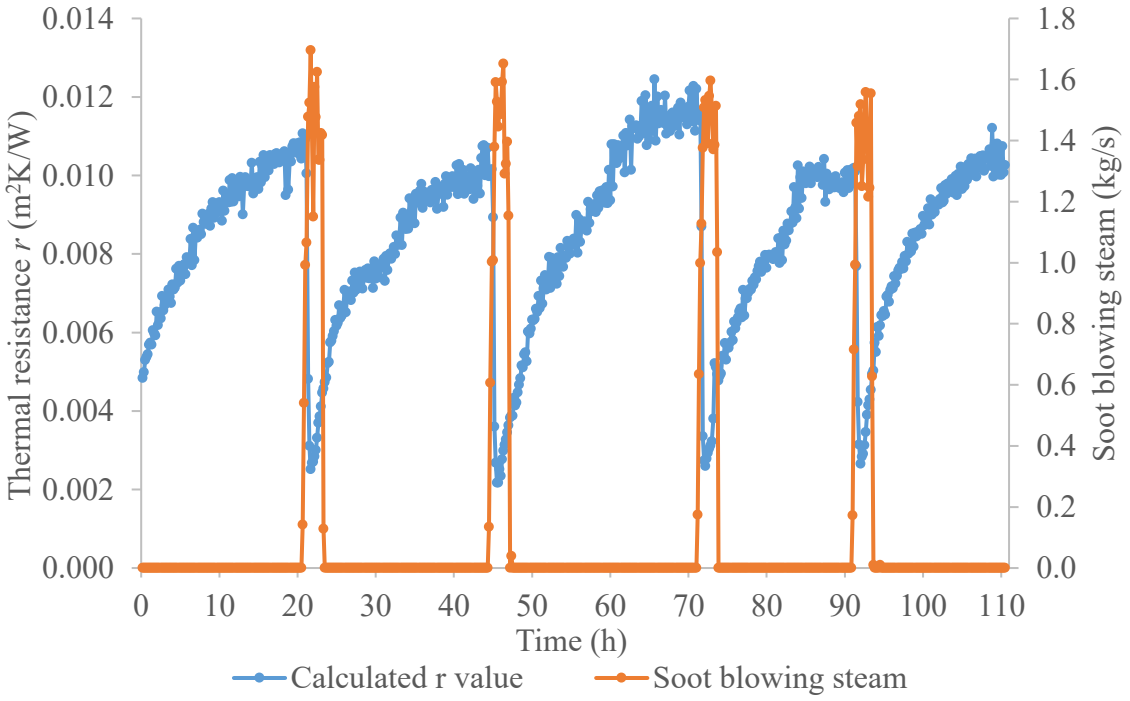

Figure 16. *Effect of soot blowing, boiler case 1, secondary superheater*

Even though the soot blowing clearly matches the r value decline phases in Figure 16, an important observation can be made during the short cleaning pulses: the r declines in a short time span, and new build-up seems to start forming while cleaning steam is still being sprayed onto the tubes. These periods will be excluded from later comparisons to maintain data handling systematic for all cases. This phenomenon could quite likely be explained by soot blowing sequencing order; the latter phase of the soot blowing pulse

could be directed at only heat exchangers that are located after the secondary superheater evaluated in Figure 16. Furthermore, the initial deposition could maybe happen despite the soot blowing, and develop into a mature deposit layer, which then comes off as a whole upon the next cleaning phase. Without any profound knowledge of the real atmosphere at the tube surface during the soot blowing, it is hard to say if this is actually true as well, in addition to the probable sequencing effect.

Another notable observation in Figure 16 can be made of the value range that the *r* falls into when soot blowing starts: there is no rising trend for the low points. Like the general effect of soot blowing, this relatively stable behavior was prominent in all calculated cases, not just boiler 1 chosen for the graph. This is an encouraging finding, because a visibly increasing trend of the low points even for a period of just a few days would indicate that either there is something fundamentally wrong in the basic calculation, or the deposition is so severe that a considerable decrease in the cleaning efficiency could be detected within days. Since this did not happen, calculated fouling rates can perhaps be studied with slightly greater confidence.

At the same time, the foregoing result induces a topic for further research: if the studied overall period continued for months instead of days, would there be a significant change in the initial thermal resistances after soot blowings? Deposit accumulation over the long haul as a physical phenomenon is an acknowledged issue, but its linkage to changes in heat transfer coefficients has been studied less. At least some of Mann's et al. results show a visible effect of the sticking, long-time deposition in their heat transfer coefficient examination, however [38, p. 28]. In this thesis, only the fouling rates for periods of about 3-24 hours were compared between the selected boilers, but a similar comparison for the long-time build-up of permanent deposits could broaden the understanding of the overall fouling phenomenon.

Some calculation cases featured individual anomalies from the previously established causal relation. For example, in boiler 4 a typical-looking surge in *r* was seen in one fouling period, even though no soot blowing sequence appeared to be going on. The occurrence of this is shown in Figure 17 at around 23 h time mark. Spontaneous shedding, which was described in Chapter 3.4, is an unconvincing explanation to this, as thermal resistance did not drop only slightly, but close to zero, leaving the actual reason to this anomaly unknown. A reverse effect, where a pulse of soot blowing seemed to be completely insignificant for thermal resistance build-up was also detected in some periods, but it was probably due to a partial blowing pulse that might have excluded the studied heat exchanger.

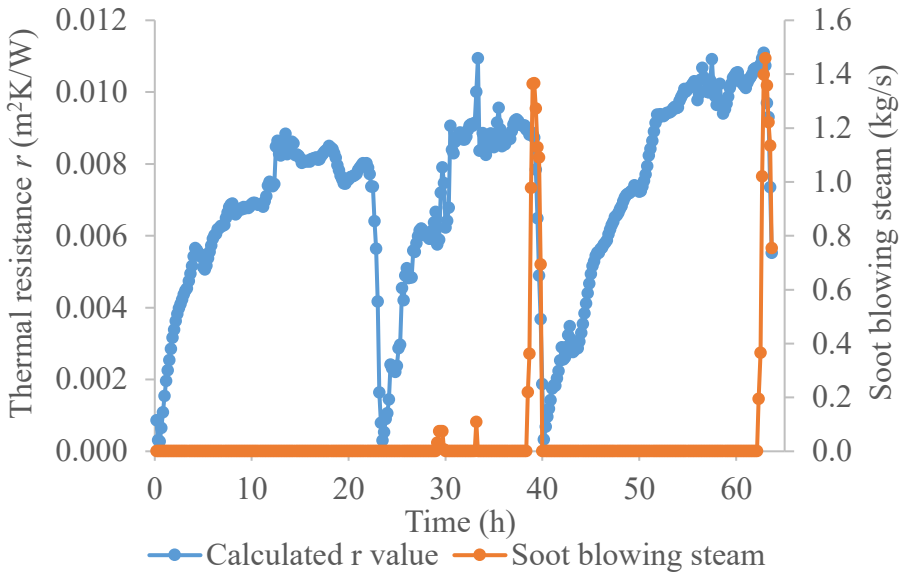

Figure 17. *Anomaly in causality between the r value and soot blowing, boiler 4*

The general conclusion that could be drawn from the calculation cases is that steam soot blowings mostly work as clear boundaries between separate thermal resistance build-up periods and can thus be regarded as the determining factor of the fouling period evaluations. With the exclusion of a few unclear exceptions, the periods separated by soot blowings were used for further studying and the fouling rate calculations.

5.3 Fouling rate calculation

After identifying the soot blowing periods, the Excel function LINEST was used to find a solution to the research question phrased as: "*How can heat transfer calculations be formulated into fouling rate examinations?"*. The outcome of this was a list of fouling rates for each marked period between the soot blowings. The length of the examined measurement campaigns varied from only five days to almost two weeks, meaning that the number of calculated rates also varied case to case. Another factor leading to different amount of calculated fouling rates per campaign was the varying duration of the fouling periods between soot blowings, which also played a role in the overall fouling rate value.

An asymptotic tendency was found in thermal resistance growth in some cases. This can be clearly seen in Figure 16 for boiler 1, where a stabilizing phase follows faster initial build-up in all visible fouling periods. This tendency was later found to have a probable linkage to flue gas pressure change alteration. The comparison in Figure 18 shows the differences between the typical thermal resistance evolutions from boilers 1-5. Adjusting all *r* value series to individual, normalized scales from 0 to 1 affects the comparability of the curve slopes, but the variation on the curve shapes is evident nonetheless: there is significant value stabilization in boilers 1 and 4, and to some extent at the end of the

fouling period of boiler 3. In addition, it can be seen that the fouling periods vary remarkably in length. The examination periods of boilers 1 and 4 count to a whole day, while the fouling period of boiler 5 in Figure 18 is only six hours long.

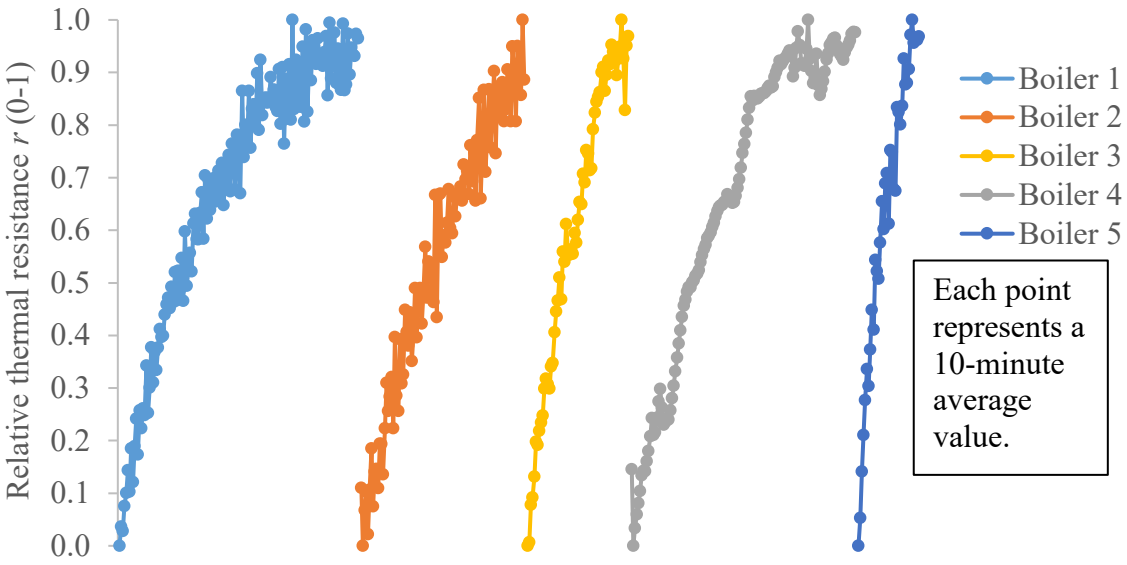

Figure 18. *Thermal resistance growth variation in the hot zones of examined boilers*

Period length variation causes a considerable issue in the fouling rate comparability between the boilers. In Figure 18, fouling does not seem to stabilize at all in boiler 5 in its own six-hour period, but neither does it stabilize in that time in the curve of boiler 1, where eventually some kind of balance is reached. It remains unknown whether the fouling would finally stabilize in the frequently cleaned boilers too. It seems clear that a more detailed comparison is needed than just a straight trendline slope determination. This was settled by dividing the fouling periods into phases of initial build-up and stabilization. For cases like boilers 2 and 5 in Figure 18, these phases were practically indistinguishable, but for asymptotic series this procedure gave more comparable data of the initial fouling rate. If only the overall slopes had been evaluated from fouling periods in boiler 1 for example, the result slope values would have been falsely low.

A determined percentage of the maximum thermal resistance for each fouling period was used as the limiting point between the initial build-up and stabilization. For example, with confirmation by visual examination of graphs, it was decided that when 60 % of the maximum r value of the examined period was reached in boiler 1, the phase was changed from initial phase to stabilizing period. This method was lacking in systematism, but without any way to determine the root cause behind the whole stabilization phenomenon, it would have been questionable to tie the limiting point with any measurement values either. The same dividing point was used for all periods per each boiler individually. Excel LINEST was still used to calculate the initial and stabilizing fouling rates, only the time ranges were adjusted accordingly. Figure 19 demonstrates the refined evaluation for one fouling period from boiler 1.

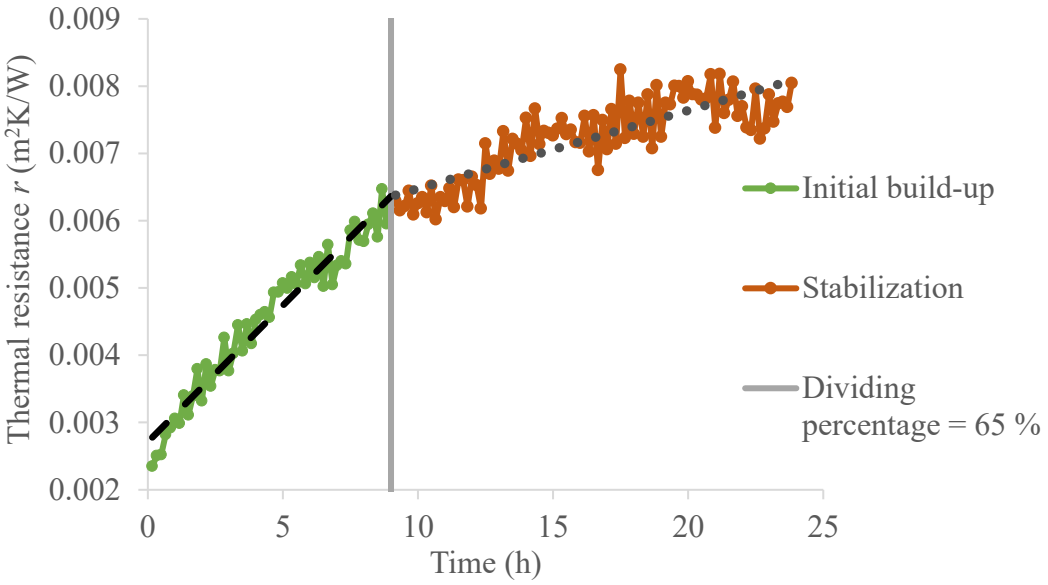

Figure 19. *Example of the division of an asymptotic fouling period, boiler 1*

The splitting method was not used for short fouling periods, like the one of boiler 5 in Figure 18, but period length was noted in the result analyses between different boilers and fuel mixtures as a relevant factor in fouling rate comparisons. The resulting fouling rates from Excel LINEST determination were not very indicative by their unit (m^2K/W per 10 minutes), but enabled making conservative further comparisons, as long as the time- and curve-related limitations discussed earlier were acknowledged.

The result fouling rates, e.g. the Rates of Calculated Build-Up (*RCBU*) were tested with *PPMCC* determination as described in Chapter 4.2. This was done to strengthen perception of the fouling rate determination quality by estimating how well the slopes describe the increase in *r* values. Average *PPMCC* values between the slopes and the *r* data sets are presented in Table 8. *PPMCC* values fall in range of 0-1, with a value close to 1 indicating that the slopes describe the calculated builds-up well.

Table 8. *Average PPMCC correlation values of calculated fouling rates*

Target slope of PPMCC examination	**Boiler case**				
	1	**2**	**3**	**4**	**5**
RCBU, overall	0.95	0.93	0.96	0.94	0.88
RCBU, initial	0.96	-	0.96	0.95	-
RCBU, stabilization	0.80	-	0.87	0.77	-

Figures in Table 8 show that the initial rates of asymptotic curves (boilers 1, 3 and 4) got slightly more precise than the overall slopes with the selected division method. The sensitivity to deviation is evident in Table 8 in the stabilization-*RCBU* values; visually examining, the data did not get as severely noisier in stabilization phases as these values suggest. More importantly though, the non-stabilizing boilers 2 and 5 produced lower *PPMCC* values than asymptotically fouled boilers 1, 3 and 4, despite their linear rise, so the whole *PPMCC*-examination did not function as a measurable asymptoticness factor at all. It only showed that Excel LINEST determination produced mostly quite good slopes of the calculated *r* data sets, thus excluding this procedure from the list of possible factors that could cause inaccuracy in fouling rate comparisons.

5.4 Correlation of calculated fouling rates with main steam power

After determining key statistic characteristics and the basis of the applied heat transfer based fouling determination, focus is moved on to research question worded as "*What is the direction of causality and strength of correlation between the calculated heat transfer values and the selected operational parameters?"*. Therefore, the parameters determined to be significant are examined next. As it was stated in Chapter 4.1, calculated fouling rates were expected to be higher under high load, as opposed to partial load conditions. However, results point out a matter that was not properly considered in the preliminary determination of effective parameters. The evaluated measurement campaigns consisted of varying test points fuel-wise, but since the campaigns were conducted in utility boilers, the overall heat and power production was held rather stable – and a load change study would not have been among the research interests of the original campaigns anyway. Figure 20 demonstrates this stability for boilers 2, 4 and 5, illustrating also the different campaign lengths. Apart from some individual peaks and boilers 1 and 3, the general fluctuations in calculated main steam power are barely over a few per cents. Moreover, even if the experienced load changes would have been significant, a direct comparison between the fouling rates and the loads would have required unaltered fuel composition to maintain some comparability on causes behind fouling.

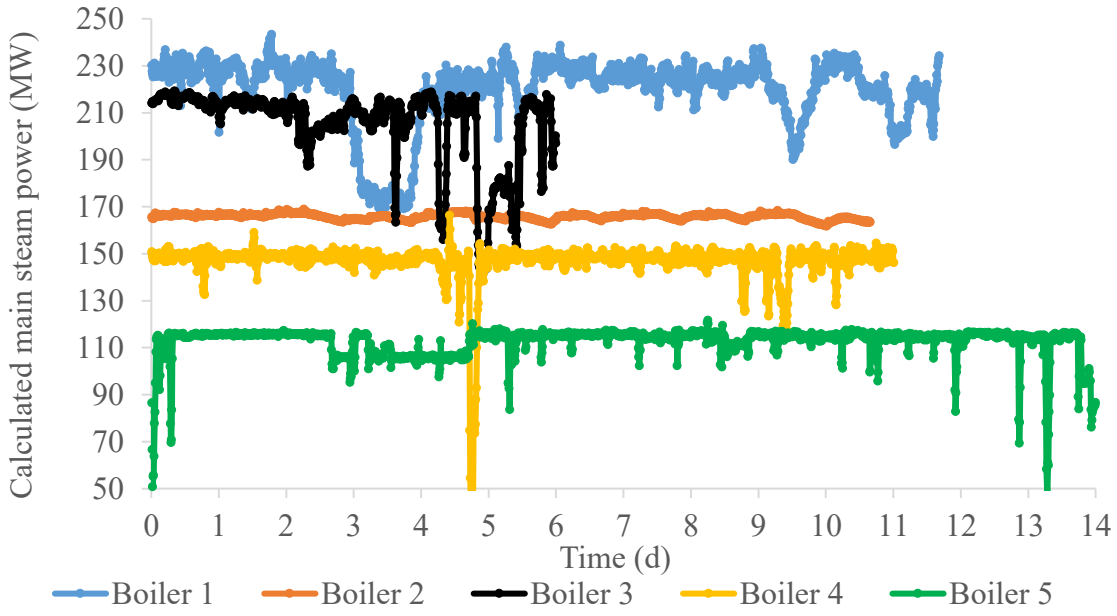

Figure 20. *Fluctuations in calculated main steam power, boilers 1-5*

Linking the fouling rate examination to the few actual load changes in Figure 20 was not as straightforward as it was initially thought. The small, temporary reductions in the steam power of boiler 2 turned out to express a negative correlation with increasing thermal resistances at the examined secondary superheater, with correlation values being less than -0.90 for some fouling periods (-1.00 being a perfect fit). This indicated an operating way of the boiler that let the steam generation drop to some extent, after which soot blowing pulse was actuated, increasing the steam power again. Although the whole operation logic would not be this simple, the firm negative correlation raised a question of whether the hypothesis of the causative nature of the main steam power changes had any foundation.

A differing reasoning could be formulated for the clear one-day deviation for boiler 1 in Figure 20. Since the original thermal resistance values did not show any anomaly despite the clearly reduced steam power on day 3 (a reduction of 21 %), the fuel mixture could have been exceptionally challenging that day – or the boiler load might not cause any effect on the fouling, unless the load change would be tens of per cents. The visible variation for boilers 1 and 3 in Figure 20 was traced to be caused by changes in the measured steam mass flow alone; temperatures and pressures remained notably stable in both cases.

Effect of the steam load adjusting procedure (which was described in Chapter 4.2)on the calculated fouling rates is summarized in Table 9, where $\Delta RCBU$ stands for the percental difference between original rates and the steam-adjusted rates. The tabulated results are from hot zone calculations. The “overall” subscript refers to the whole fouling period, and initial and stabilization stand for the two possibly distinct phases of an overall period respectively. Interestingly, despite boiler 3 showed some significant downward troughs in calculated steam power in Figure 20, the adjustment did not make a big difference in

the *RCBU* values. In boiler 1 however, the initial and stabilization rates got changed quite a bit during the load reduction seen in Figure 20, affecting the average difference considerably too. Moreover, the calculated steam power appeared to fluctuate considerably in boiler 1, highlighting the big difference of initial and stabilized rates in Table 9.

Table 9. *Average effect of steam power adjustment on fouling rates*

Object of average comparison	Boiler case				
	1	**2**	**3**	**4**	**5**
ΔRCBU, overall	6.6 %	2.2 %	5.3 %	0.8 %	4.75 %
ΔRCBU, initial	14.2 %	-	5.5 %	2.7 %	-
ΔRCBU, stabilization	44.6 %	-	8.5 %	6.8 %	-

In conclusion, the causality between the slight load changes and fouling was not clear with available measurement data. As stated earlier, boiler 2 appeared to show a specific effect of steam power decreasing along a progressing fouling period, not vice versa. The comparison in Table 9 does not depict the actual fouling changes of boiler load fluctuation in any way – it only demonstrates the differences caused by the decided adjustment for fuel mixture comparison. Larger load changes with stable fuel mixtures would probably have produced more deviating and therefore informative results in the stand-alone load study.

As mentioned earlier, direct fuel load values would have been preferable for the load study, should they have been reliable. Comparison of automatically calculated fuel loads and calculated steam power values revealed that the fuel load measurements were surprisingly close to steam figures in boilers 2 and 4, and correlation was strong in boilers 1 and 3 too. However, standard deviation of fuel load numbers was 84 % higher than that of steam power in boiler 1 for example, and DCS log from boiler 5 did not include any kind of automated fuel load calculation values, so the selection of steam power for load effect examinations instead of fuel load was sensible after all.

5.5 Correlation of fouling rates with fuel mixture variation

Relation between deposition and the fuel composition was presented in Chapter 3, highlighting the importance of alkalis (Na, K) and Cl. When putting the fuel mixtures in order by increasing combustion difficulty, these components have a significant role. In close relation to these components, the challenging nature of biomass and waste (or recovered) fuels is recognized in good consensus [22], [24], [39], [48], [49], [61], [68]. Therefore, it was expected that the fuel mixture variation would be clearly visible in the fouling rate examination. Fired fuel feeds were categorized coarsely according to the classification

presented in Chapter 2.4. Coal and peat were expected to be almost easy or neutral in terms of fouling, waste- and agriculture-based fuels were seen rather demanding and woody biomass was deemed to lie somewhere between the two extremes.

The fuel mixture varied in all boilers except number 2, in which only a moderately challenging recovered fuel was combusted. In boiler 2 the only fuel-related and measured variable was the limestone feed for sulfur reduction, which was stopped for a couple of test points. Figures 17-19 show how *RCBU*'s change by changing fuel mixtures in boilers 1 and 4. Fuel mixtures could only be selected from test point days, for only then an acceptable validation of the mixture shares was performed.

The brief inclusion of the fuel variation here does not depict the actual outcome of the confidential internal project; insightful overall results would require delving deeper into fuel feed composition, and this would have been outside the scope of the thesis. The presented figures also lack some of the test points and fuel mixtures, because only the most representative ones were chosen for display. Even these points give only a rough indication of the effect of fuel.

Coal, peat, wood, and a recovered fuel were fired in boiler 1. The considerable load change in boiler 1, visible in Figures 11 and 16, takes place in fouling period 2 here in Figures 17-18. In that specific period, the load adjustment seemed to emphasize initial rate in an expected manner, while influence on stabilization phase seemed a bit odd. Despite the steam adjustment described in Equation (13) highlighted reduced loads, not elevated, the adjusted stabilization-*RCBU* was smaller than original *RCBU* during reduced load in period 2. However, at the end of fouling period 2, ergo during the stabilization phase, the steam power started to normalize again, which could perhaps explain the opposite effects on initial and stabilization phase fouling rates. Other notable observations from both figures include the overall and initial *RCBU* peak values occurring at highest share of recovered fuel in period 2, and elevated initial *RCBU* values in periods 3 and 4 over period 1, when coal has been changed to a relatively large share of peat.

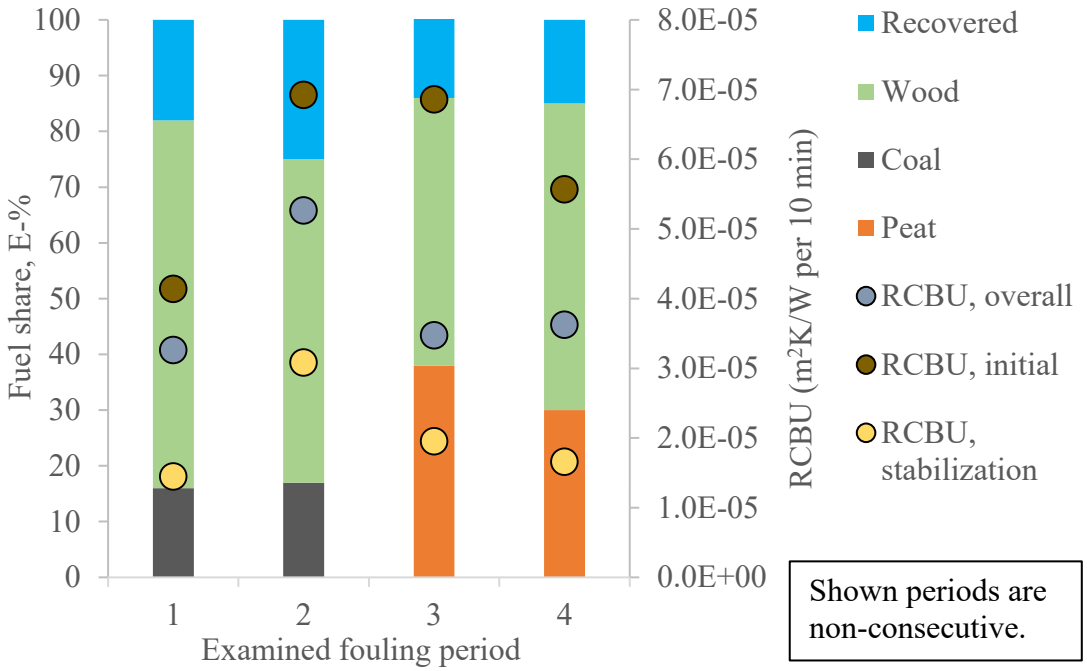

Figure 21. *Fuel mixture variation with untreated RCBU values, boiler 1, hot zone*

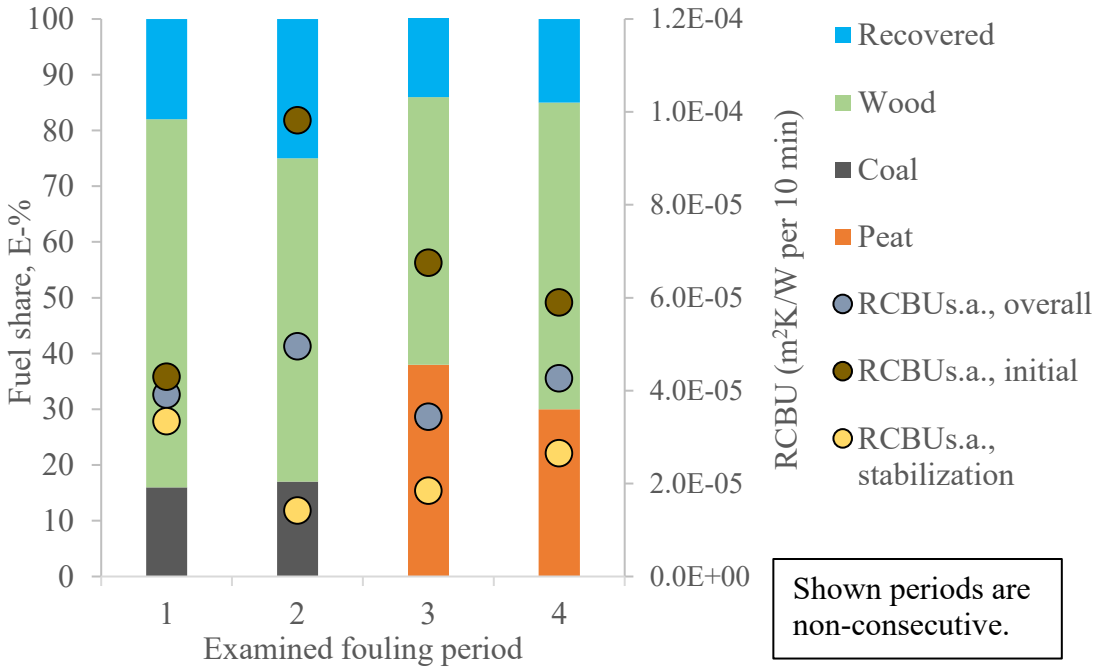

Figure 22. *Fuel mixture variation with steam load adjusted RCBU values, boiler 1, hot zone*

Boiler 4 showed the most interesting results in terms of fuel mixture. The general shape of thermal resistance build-up curves in boiler 4 had a bit more deviation than those of boiler 1, as it was showed in Figure 18, but the fuel feed variation was a bit simpler, allowing for easier examination. Figure 19 contains the untreated *RCBU* values for four of the examined fouling periods in boiler 4.

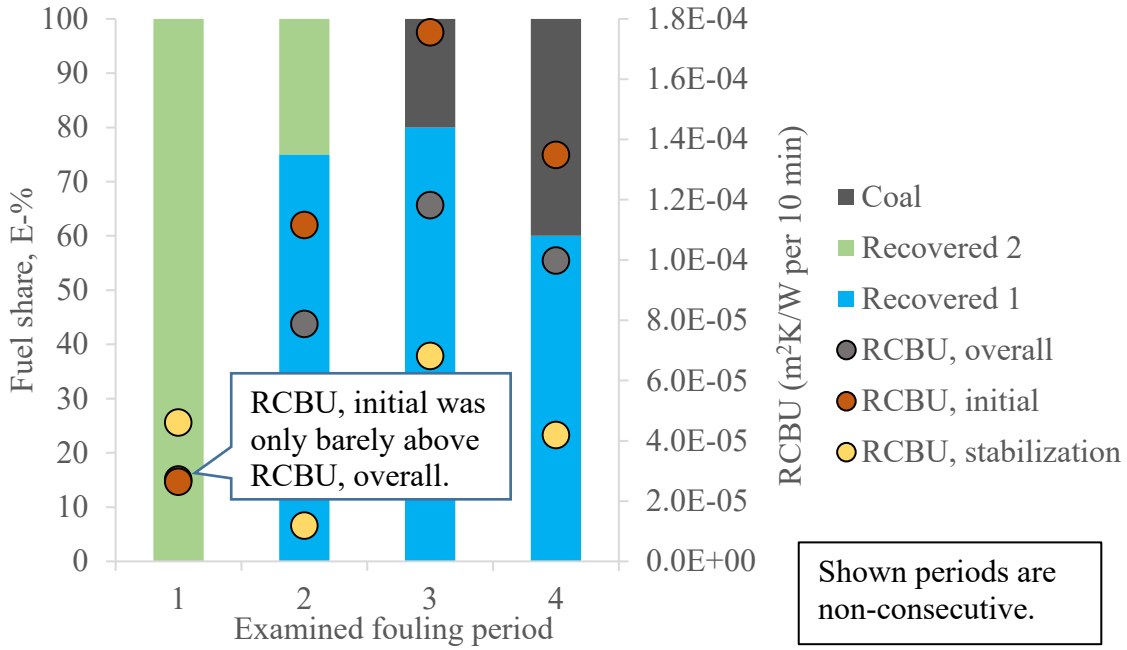

Figure 23. *Fuel mixture variation with untreated RCBU values, boiler 4, hot zone*

Despite the rather random looks of Figure 23, some conservative observations can be made. Despite both being named as recovered feeds, the recovered 1 and recovered 2 fuels were differing in composition and expected difficulty. Looking at the overall and initial *RCBU* lines, the peak values were calculated from the day of largest share of tough recovered fuel (1), whereas the lowest values were from period 1, when the fuel consisted entirely of recovered fuel that was determined to be the easier of the two waste-based feeds. Periods 2 and 4 show surprisingly similar values for initial and overall *RCBU*'s, even though the other recovered fuel is changed to supposedly trouble-free coal. As the main steam power was rather consistent in boiler 4, the differences ought to relate mostly to fuel – and hence only the non-adjusted *RCBU* values were presented here.

Although deposition dominance by alkali chlorides has been pointed out repeatedly, the differing temperature zones must be considered when rating the difficulties of individual fuels for each boiler case – meaning that a high alkali and Cl content does not necessarily dictate the worst fouling, if the temperature range is mild enough. In boiler 4, worst fouling rates were calculated with combination of recovered fuel 1 and coal, even though their combined alkali content was not very severe, underlining the excessive simplicity of shown fuel evaluation in Figures 17-19.

Fouling rate behavior of the stabilization phases in boiler 4 appeared to be unstable, because calculated thermal resistances showed extended rise for some periods even after the determined stabilization point. This clearly happened at period 1 in Figure 23, for instance, where the extended increasing led to stabilization-*RCBU* being higher than initial rate. Division point of 75 % (of period-related maximum *r* value) had to be used for boiler 4, as opposed to the 60 % of boiler 1, so the stabilization took relatively longer in boiler

4 to begin. The average range of the overall *RCBU*'s was also higher in boiler 4 than in boiler 1, despite the cooler temperature zone, which indicates that the deposition in general was more severe there.

Calculations on boilers 3 and 5 showed more indefinite results fuel-wise. The lowest overall *RCBU* value in boiler 3 was detected along highest share of wood, which was possibly the easiest fuel in there. While variation between wood and coal was considerable, the amount of challenging waste-type fuels was kept rather stable, so it is possible that the *RCBU*-fuel comparison was affected by too consistent fuel mixture, as it seemed to happen in boiler 1 to some extent.

The measurement campaign of boiler 5 covered various challenging agrofuels, but the test points lasted even just two hours, so reliable information of the average fuels during the fouling periods was not thoroughly available. However, if the shortest and therefore the most unreliable periods were ruled out of examination, the results showed the same finding than with boiler 3; lowest initial – which in boiler 5 was also overall - *RCBU* occurred when the fuel mixture consisted mainly of wood, e.g. the easiest fuel in the measurement campaign there. Higher *RCBU* rates were found for mixtures containing varying agrofuels, none of them standing out clearly as being the worst.

When interpreting the figures, there are some important notices to keep in mind: first, stable fuel shares of the short test points were assumed to be maintained for the whole longer fouling periods, given that the test point period was deemed long enough for any evaluation in the first place. Second, the difficulty of each separate fuel feed could vary even within the campaign, especially with waste fuels that can be substantially heterogenous. Varying use of additives, such as limestone, also altered the flue gas composition.

5.6 Correlation of thermal resistance with flue gas pressure gradient

Unreliability of direct volumetric flue gas flow measurement from the stack led to the application of the LMTD method in thermal resistance calculations instead of NTU, eliminating the need of the flue gas flow measurements. Original objective was to use the flow measurements also to calculate flue gas velocities at studied heat exchangers. As that turned out to be a flawed way, the correlation between the pressure difference and the resistance r was studied instead. It should be noted that focus here is on the change of the gas-side pressure difference (Δp), not on the Δp value itself, which is a natural occurrence in heat exchangers even without the fouling phenomenon [63, pp. 1076–1091].

The Δp was a direct measurement calculated by DCS. The zone between the two pressure measurement points covered more than the studied heat exchanger in all cases, but this was not assumed to have any significant influence in the comparability. Figure 24 shows

how *Δp* over secondary and primary superheaters (SSH and PSH) varied along thermal resistance build-up in boiler 1.

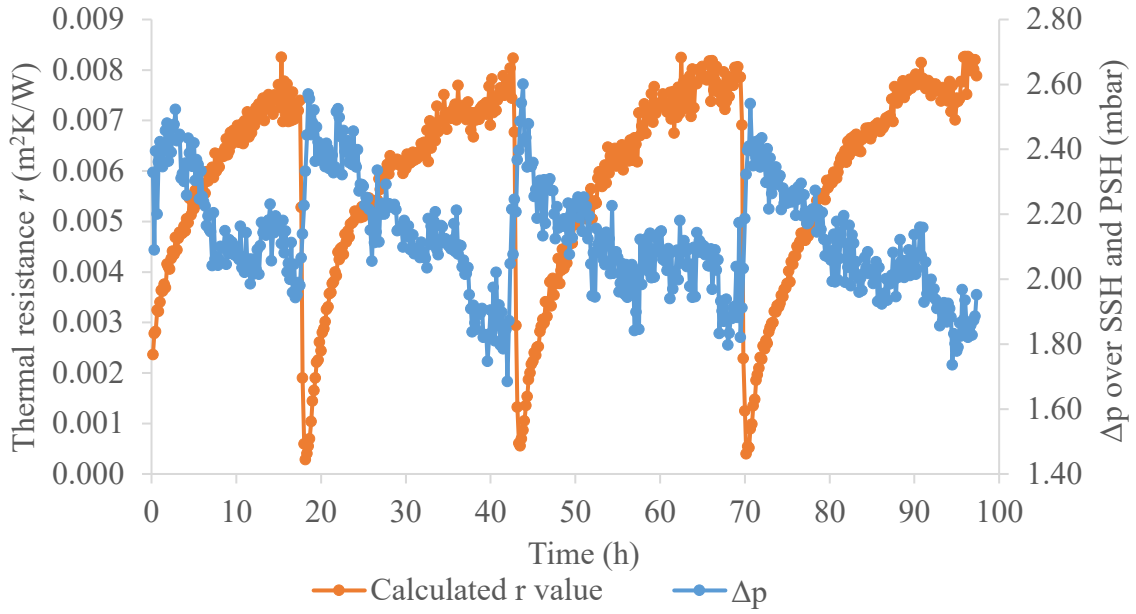

Figure 24. *Correlation between Δp and calculated thermal resistances, boiler 1*

For the time section selected to Figure 24, a clear correlation can be seen between the pressure difference and thermal resistance, despite the considerable deviation visible in the *Δp* measurements. For this period, a negative correlation value of -0.795 was calculated, indicating a strong relation between thermal resistance build-up and *Δp* decrease. However, the strong correlation does not tell anything about the causality yet. In principal, a decrease in *Δp* refers to change in the flue gas flow velocity, but the velocity change could be caused either by deposit layers slightly constricting the flow channels, or by a change in the flow earlier before the studied duct area. Nevertheless, the correlation in Figure 24 strongly suggests that in this case the first mentioned phenomenon takes place.

A correlation similar with boiler 1 could not be found in boilers 2, 3 or 5. In boiler 2, sharp downward peaks in *Δp* were identifiable for every soot blowing, but during the fouling periods, a relatively steady level was quickly reached again and no systematic change along cumulative deposition could be observed. Therefore, the statistical correlation calculations were not performed. A couple of sudden surges in *Δp* values matched temporally with soot blowings in boiler 3 too, but otherwise the pressure measurements did not point out any connection to fouling in boiler 3 either. The required measurements lacked completely from boiler 5, so the *Δp* examination could not be done.

Interestingly, boiler 4 produced quite opposite results to those of boiler 1. The correlation was strongly positive, instead of the reverse one seen for boiler 1 in Figure 24. For the selected period in Figure 25 for boiler 4, the positive correlation value was 0.940. The opposite shape of *Δp* for boiler 4 than for boiler 1 raised a question of which curve was

more logical. The pressure gradient should increase by increasing constriction of the flow channel, so the *Δp* shape in Figure 25 seemed to make more sense. It was reasoned together with a process engineer that the pressure change measuring instrument could simply have been installed the wrong way around in boiler 1. As with boiler 1, the correlation itself in boiler 4 does not reliably prove the causal direction between the two phenomena, but indicates that a limit in the change of the pressure gradient is reached alongside the asymptotic deposition.

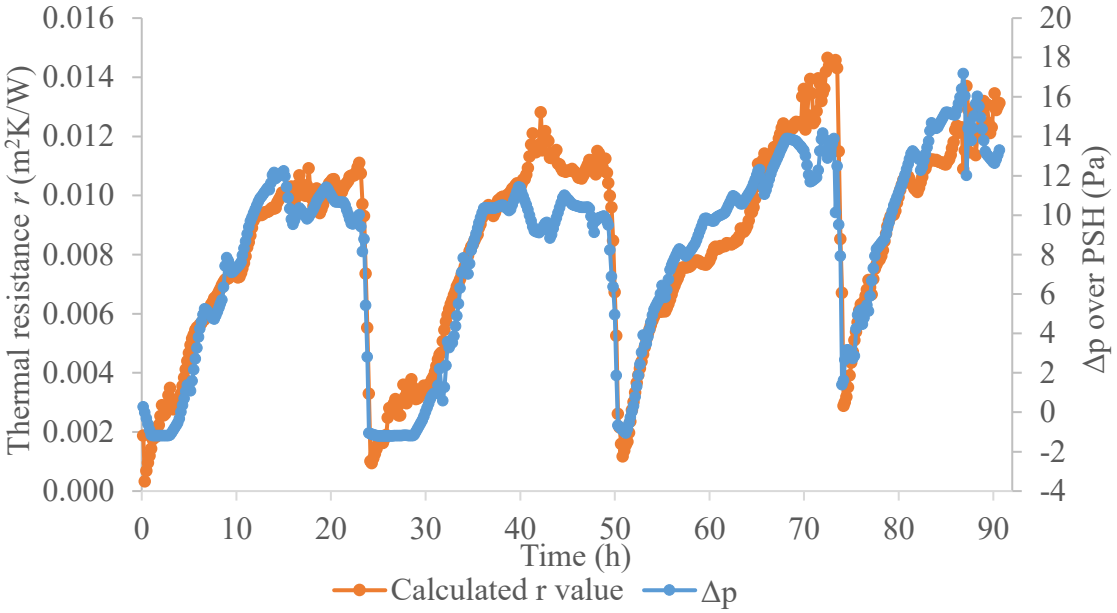

Figure 25. *Correlation between Δp and calculated thermal resistance, boiler 4*

Strictly speaking, the found correlations from boilers 1 and 4 are of questionable value. Even though the relation exists, it does not prove whether the change in pressure difference or flue gas velocity alters the deposition build-up. An accelerating flue gas could influence the inertial impaction properties of ash particles, as described in Chapter 3.2.1, but it is also possible that the changes seen in Figures 20-21 are too small to be related to this. In any case, the changes in flue gas flow properties give one proposal in explaining thermal resistance asymptoticness of boilers 1, 3 and 4: after a shift in principal deposit formation method from sticky diffusion to inertial impaction, the flue gas velocity might act as the limiting factor of further deposition by inhibiting impaction after a certain point. The ample ash content in the fuel mixtures of both boilers 1 and 4 support this view, but no critical assumptions of the deposition physics should be drawn from these results. In any case, physics-related explanation for the stabilization seemed to make more sense here than the Fe and Ca -emphasizing conclusion that Namkung et al. [43] had for the asymptotic results of their coal fuel study.

5.7 Comparisons between hot and cold zones and separate boilers

Final research question to be considered was expressed as "*What kind of relations do the calculated fouling rates pose between different temperature zones within each boiler, between different evaluated boilers, or with other rate determinations?*". Earlier comparisons in Chapters 5.4-5.6 focused completely on hot zone, excluding speculations between the different temperature zones. This was because deposition was expected to be greater in the hot zone in general, the LMTD calculation was assumed to be more precise for heat exchangers of larger temperature differences, and because for some cases, the cold zone thermal resistance calculations were simply unsuccessful. For example, while the increasing trend in thermal resistance was clear in boiler 1 for the secondary superheater, the corresponding calculation for economizer produced an almost straight line, but with greater deviation. However, it is also a possibility that the deposition truly took place mainly in the hot zone, and negligibly in the cold zone in boiler 1. This unclear *r* evolution in cold zone is illustrated in Figure 26 below (gray line), with steadily behaving *r* curve for the hot zone (blue line) included for comparison. Time span in Figure 26 is the same that was used in Figure 16.

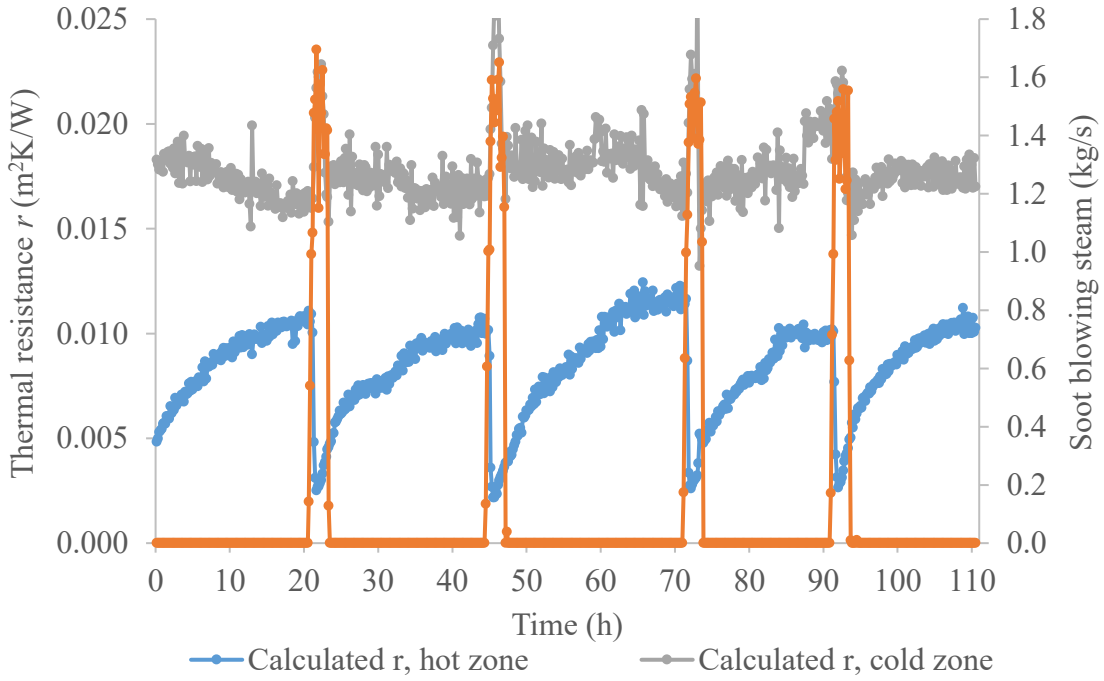

Figure 26. *Thermal resistances of hot and cold zones, boiler 1*

For the reasons explained above, the temperature ranges of the studied heat exchangers should be considered when interpreting the hot and cold zone comparisons of thermal resistances and *RCBU*'s. Table 10 lists average flue gas inlet temperatures for all evaluated cases. The listing shows that in boilers 3 and 4, the flue gas temperature difference between heat exchangers selected to present hot and cold zones was quite small.

Table 10. *Average flue gas inlet temperatures for the hot and cold zone heat exchangers*

Flue gas temperature zone	**Boiler case**				
	1	**2**	**3**	**4**	**5**
Hot zone, flue gas inlet T (°C)	879	811	529	467	565
Cold zone, flue gas inlet T (°C)	458	444	461	341	-

The studied heat exchangers could not be selected from exactly matching temperature ranges, especially on the hot zone, because required measurements were not available for all heat exchangers. Moreover, boiler 4 had an empty pass between the CFB cyclone and the first convective heat exchanger, which explains the lower temperatures in both zones. Also, the measurement points for the hot zones of boilers 1 and 2 were directly after the cyclones, so the actual flue gas temperature at the superheater inlets must have been lower.

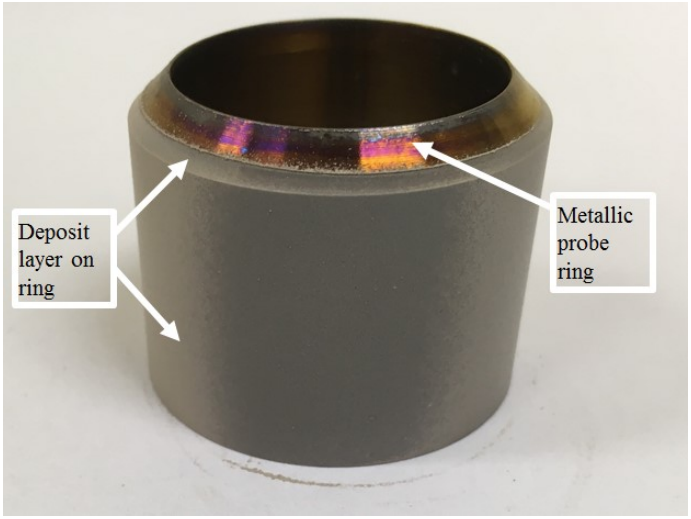

Figure 27 *A deposit probe ring from the hot zone of boiler 3*

Research targets included fouling rate comparisons against other related determinations. Practically, the relevant other determinations meant mass build-up examinations from deposit probes that were used during the measurement campaigns. A weighed probe ring from boiler 3 hot zone can be seen in Figure 27, showing an evident, firm deposit layer on the metal piece after a two-hour exposure to flue gas. Deposits on the actual heat exchanger tubes can be different by appearance though, since the flue gas flow pattern within the tube elements may be different from that around a single probe tube.

Calculated thermal resistances over a period of approximately two days in boiler 2 are presented in Figure 28 for hot and cold zones. Interestingly, the resistance values of the cold zone are generally higher than those of the hot zone and the overall *RCBU* numbers

for the selected fouling periods are higher in the cold zone too. This result could be explained by a fundamental difference in the calculation accuracy between superheaters and economizers, or by actual increase of deposition in the colder zone. It is noteworthy that the varying reference heat transfer coefficients (U_{clean}) can also put hot and cold zones in very different positions in terms of *r* value credibility. The abnormal peaks seen in cold zone *r* values did not affect the *RCBU* determination, as they occurred during soot blowing, so they cannot explain the difference of the *RCBU* values.

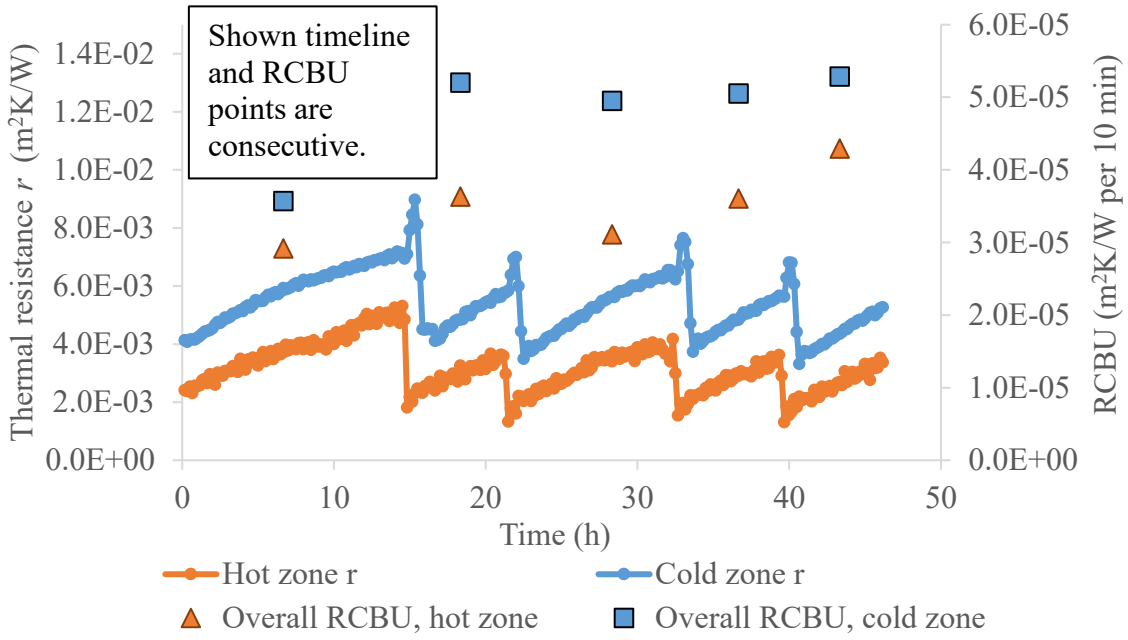

Figure 28 *Comparison of r and RCBU values in hot and cold zones, boiler 2*

During the measurement campaign of boiler 2, deposit probes were used and the formed deposits were analyzed. The findings from chemical analysis of the deposits did not support the hypothesis of more severe fouling in cold zone, if focus was kept on alkali and Cl contents. However, actual fouling rates were not calculable from probe ring masses. Results from other boilers were hence needed to understand better the hot and cold zone difference and cold zone calculation validity.

Examination between hot and cold zones in boiler 3 produced similar results with boiler 2 in that the cold zone *r* values were generally higher than in the hot zone. In boiler 3 though, the *RCBU* rates were mostly higher in the hot zone. This result matched the deposit probe ring mass accumulation determinations from the original measurement campaign, albeit the comparative probe to represent the cold zone was located closer to air preheaters than the economizer that in turn was examined here. The hot zone probe on the other hand, ring of which was seen in Figure 27, was placed closely before the examined superheater.

Unfortunately, cold zone calculations from boilers 1 and 4 did not yield any additional reference data, because for an unknown reason the *r* values did not follow the build-up

trend during the fouling periods thoroughly. Boiler 4 had a couple of sensible build-up phases, but overall relation with soot blowing remained rather random. Clearer increases were seen generally in boiler 4 cold zone than in boiler 1 though. The same data-related issue that disrupted the fuel and steam load comparisons also seemingly occurred here: despite some connection with alternative measurements, the data available for final comparison of hot and cold zone fouling differences was not sufficient to gain good statistical confidence in the results.

Transverse and longitudinal tube pitches can also play a role in the hot versus cold zone comparisons. Typically, the longitudinal pitches are tightened along cooling flue gas [52, p. 212], and this basic principle also occurred in all of the examined boilers. Tight tube spacing in the cold zone might have explained the differences, if cold zone *RCBU*'s were consistently higher. As this did not happen, it remained unclear as to what were the overall fouling impacts of the tight cold zone tube spacing and of the more challenging hot zone temperatures respectively.

If the applied thermal resistance determination was correct, an explanation for the unexpected cold zone *r* stability in boiler 1 or the time disruption of fouling phases in boiler 4 could be sought from tube pitch differences between boilers 1-4. Comparison of transverse tube pitches in these boilers showed similar values for all studied economizers in boilers 1-4 though, so at least tube spacing was not the deviating factor mitigating cold zone fouling or at least disturbing periodic nature of *r* evolution in boilers 1 and 4.

A brief boiler-to-boiler comparison was conducted only for the hot zones, as some cold zone results were lacking or indecipherable, as described above. Overall *RCBU* figures were used to determine broad differences in the calculated fouling rates between the boilers and they are presented in Figure 29 in original forms, e.g. without any steam adjustments. When interpreting the figure, it should be kept in mind that burned fuel mixtures were influential to changes within each boiler: for example, the increase seen for boiler 5 in Figure 29 was assumedly fully related to fuel mixture changes, instead of fouling worsening randomly towards the end of the measurement campaign.

The main finding in this comparison is that the calculated overall fouling rates fell into a rather compact range – apart from boiler 4 – despite the asymptotic curves in boilers 1, 3 and 4. A few last data points of boiler 2 were ruled out from Figure 29 for the sake of representation, but the excluded points had values only within the visible range of boiler 2 in the figure. Boiler 4 stands out significantly, indicating a strong fouling tendency, and this result agreed with opinions of the people who were involved in the original measurement campaigns and with the probe ring mass accumulation determinations.

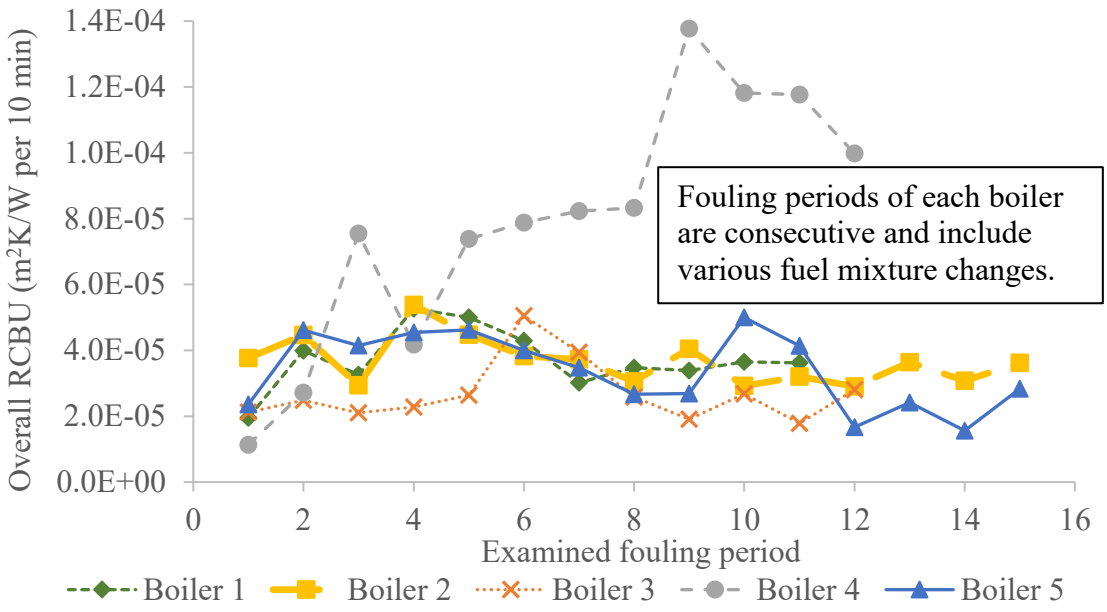

Figure 29 *Comparison of overall RCBU figures of hot zones in boilers 1-5*

Interestingly, conclusions from Figure 29 make sense fuel-wise, because the main constituents in the fuel mixture of boiler 4 were two types of recovered fuels. In all the other boilers, differences could probably be explained by other factors to at least some extent – despite having distinctive fuels – but for boiler 4, the somewhat extreme fuel feed seems to have a real effect on fouling rates. This finding agrees with Eklund's and Rodin's survey on a few Swedish boilers, where the boilers fired with recovered fuels stand out for having elevated levels of deposit accumulation [15, p. 73].

5.8 Key findings, issues, and targets for development

In conclusion, the results of the computational part were a bit mixed. The primary target – to examine the applicability of heat transfer calculations as a method of fouling identification – was met, but secondary target of finding correlations with operational parameters turned out to be more uncertain, the correlations being non-existing at worst. Some connections could be found still, with flue gas pressure change especially showing strong correlation with calculated deposit build-up. On the other hand, many possible factors causing the variation and uncertainty were noticed, along with some enhancement suggestions. Moreover, one should keep in mind that suppressing operation of a complex full-scale superheater or economizer into simple figures of inlet and outlet temperatures and flows forms a very different research subject than a small test tube in lab-scale applications from accuracy point of view.

The original case selection got significantly reduced when it came out that the DCS measurement points were insufficient in amount or in placement in half of the originally intended boilers. As each of the evaluated boilers produced meaningful information, a larger number of total evaluated cases would have increased the statistical confidence of

the findings. Especially the fuel mixture comparison would have benefited of stable results from more boilers burning similar kinds of fuels.

Calculation-wise, the computed thermal resistance accuracy could be improved mainly by better DCS data precision and refined reference state determination. The flow measurements probably could not get much better, but the temperature measurements would be more accurate, if the permanent thermocouples would be located closer to the centerline of the flue gas duct. Cost- and performance-wise this might not be a viable option, though. Also, the available temperature measurement points should have preferably always been close to the heat exchanger inlets and outlets, but this objective could not be followed completely. In addition, accuracy was affected by how the studied superheaters and economizers were treated as counter flow heat exchangers, while the actual structures can have some features from mixed flow exchangers too.

As described before, the reference state was retrieved from process design modelling results. While the heat surface area would stay the same, the reference heat transfer coefficient for clean state would have benefited if there was a model case matching the average process parameters from the examined measurement campaigns. For seeing the approximate correlations between the selected characteristics and fouling rates this probably would not have helped much, but thermal resistance values could have got a bit more accurate. Because of the limited value for the research targets here, new complex process modelling cases were not formulated, but the closest equivalent cases were used.

It should be noted that the formulation of thermal resistance r in Equation (12) leads to a situation where greater error is caused by unrealistically high reference heat transfer coefficient U than what a low estimate would produce. In other words, if the actual clean tube U was higher than estimated, the proportional incorrectness in the r determination would be limited by the functioning of Equation (12), whereas a much lower actual clean state U would change the results a bit more significantly.

A brief sensitivity analysis to clean state reference-U value variation is presented in Table 11 as percental differences between formed $RCBU$ rates in boiler 1, showing slightly larger inequality if U is lowered. The comparison indicates that the U_{clean} determination is rather critical for the $RCBU$ accuracy and this might also have a significant effect on boiler-to-boiler comparison, which was seen in Figure 29. It can also be deduced that a distinction between modelled and actual clean state U's would be more harmful in cases were the values themselves are low, because then a small change would perhaps lead to a bigger percental error.

Table 11 *RCBU sensitivity to clean state U-value variation, boiler 1, hot zone*

Tested difference to reference state *U*, W/m^{2}K	-5	-2	+2	+5	+10
Average percental difference of overall *RCBU*	-3.86 %	-1.42 %	+1.28 %	+2.97 %	+5.32 %

In general, the calculated thermal resistances followed clear, increasing patterns in most of the fouling periods, but the *RCBU* determination suffered from the inconsistent soot blowing timings. Fully comparable results would have required minimal alteration in the fouling period durations and considerable length for the fouling periods of all cases, in order to see if the asymptotic behavior existed. For the fuel mixture study, the original campaign test points were unfortunately short and unique. Acceptable statistical confidence could have been reached perhaps if same fuel feed was fired for several fouling periods, but in some case the fuel mixture was changed even within the same period, impeding the *RCBU* correlation with fuel. Even so, some estimations of the severity of high waste share in the fuel mixture could be obtained.

6. CONCLUSIONS

Fouling of superheaters and economizers in the convective pass of a fluidized bed boiler is a major issue that reduces the efficiency of the boiler. It is caused by fly ash particles that drift along the flue gas and may stick onto heat transfer tubes. Composition of the fly ash is dependent on the fuel feed, and fluidized bed boilers are often used to fire increasingly challenging low-quality fuels. Therefore, the fouling problem can be more serious in BFB and CFB boilers than it is in PC boilers. The problem can be minimized by soot blowing devices, boiler design solutions, process parameter optimization, and careful fuel selection.

Fouling is driven by a few transportation mechanisms, including diffusion, inertial impaction and thermophoresis. Propensity of sticking ability of the ash is seen to be controlled by the amount of molten phase in it, while the melting phase temperatures depend on the ash composition. Na, K and Cl are commonly considered as the most significant elements that together can lower the ash fusion temperatures, and are therefore significant for fouling at high temperatures.

Fouling tendency has been evaluated by various methods, including fuel-based indices, chemical equilibrium calculations and CFD modellings at least. All these methods have their advantages and drawbacks: indices produce quick but incomplete estimations, while CFD models can be quite accurate, but complex and time-consuming. Existence of deposition can be examined by observing mass build-up of tube elements or heat transfer deterioration. These yield data of actual fouling with a possibility of real-time validation, but cannot be used as predictive evaluation mechanisms.

The computational part of the thesis focused on heat transfer examination of superheaters and economizers. The main purpose was to examine fouling via calculating the thermal resistance of formed deposits on tube elements. This work was part of an internal project at Valmet Technologies, aiming to produce fouling propensity and rate data from earlier measurement campaigns conducted in four CFB and one BFB boilers. DCS data was prehandled and imported into an in-house tool that utilizes the LMTD method to calculate thermal resistance for each given time point. Evolutions of resulted resistances over time were then formulated into estimations of fouling rates.

Research targets were to show applicability of the heat transfer calculations and to find correlations between operational parameters and calculated thermal resistances and fouling rates. Studied heat exchangers were divided into hot and cold zones, based on flue gas temperatures and heat exchanger types. Calculation showed clear rising trends in thermal resistances between soot blowing pulses for 7 of 9 evaluated exchangers. Anomalies not connected to soot blowings were only detected in a couple of the fouling periods.

Cleaning actions dropped thermal resistances to approximately same initial levels for each period per examined boiler. Clarity of the increasing trends indicated that the calculations expressed fouling phenomenon itself quite reliably, but the accuracy of each calculated resistance value was affected by various factors, such as flue gas temperature measurements and clean state heat transfer coefficient determinations.

Correlation and direction of causality with main steam power, fuel mixture and flue gas pressure gradient were studied as secondary research target. The steam power changes were mostly small, and did not seem to cause clear disruptions in thermal resistances. Steam power also was not the optimal figure to describe load changes on the flue gas side, leaving this comparison a bit uncertain in general. Nevertheless, the small changes were seemingly the actual cause for weak correlations. The mixed results of fuel mixture correlations expressed some uncertainty for test points that were fairly similar by the fuel mixture feed shares, but on the other hand, the easiest and most challenging fuel feeds occurred with smallest and largest fouling rates in some boiler cases. More test points with same fuel feed and more substantial variation between easy and challenging mixtures would have been beneficial for result confidence. In conclusion, correlations with fuel variation hinted that fuel feed variation caused changes in calculated fouling rates, but correlation strength was not high.

The best correlation between the examined parameters and thermal resistances was found in flue gas pressure gradient along the studied heat exchangers in two of the boilers. An asymptotic behavior of the thermal resistances – found in three of five studied boilers – was also seen in both available and correlating pressure change data. This indicated that the asymptoticness in thermal resistance curves meant real reduction in the deposit build-up. The stabilization effect was perhaps caused by flue gas flow characteristics, as the accelerated flow could have halted further fouling via deposit erosion.

Other brief examinations included hot and cold zone, boiler-to-boiler, and deposit probe comparisons. Juxtaposition between fouling rates in hot and cold zones did not produce clear conclusions of differences between the zones, and thus the assumption of greater fouling in hot zone could not be confirmed. Cross-boiler comparison revealed rather steady levels of fouling rates, as only one boiler deviated significantly from others, expressing an elevated fouling level. This deviation was arguably caused by challenging fuel. Fouling rate matching with the few available deposit probe determinations was clear in a couple of cases, but not consistently in all.

Altogether the main objectives of the work were reached. Insight of the chosen heat transfer based fouling examination method was gathered, and major limitations or parameters that are crucial to result accuracy were identified. A more extensive set of data would have been desirable, which is a fixable issue in future, if the conducted work on fouling examination is applied to forthcoming measurement campaigns at Valmet Technologies.

REFERENCES

[1] M. S. Abd-elhady, C. C. M. Rindt, J. G. Wijers, A. A. van Steenhoven, Particulate fouling in waste incinerators as influenced by the critical sticking velocity and layer porosity, Energy, Vol. 30, 2005, pp. 1469–1479.

[2] M. S. Abd-elhady, S. H. Clevers, T. N. G. Adriaans, Influence of sintering on the growth rate of particulate fouling layers, International Journal of Heat and Mass Transfer, Vol. 50, 2007, pp. 196–207.

[3] E. J. Anthony, Fluidized bed combustion of alternative solid fuels; status, successes and problems of the technology, Progress in Energy and Combustion Science, Vol. 21, No. 3, 1995, pp. 239–268.

[4] R. Backman, M. Hupa, E. Uppstu, Fouling and corrosion mechanisms in the recovery boiler superheater area, TAPPI Journal, Vol. 70, No. 6, 1987, pp. 123–127.

[5] G. Baernthaler, M. Zischka, C. Haraldsson, I. Obernberger, Determination of major and minor ash-forming elements in solid biofuels, Biomass and Bioenergy, Vol. 30, No. 11, 2006, pp. 983–997.

[6] N. El Bassam, Handbook of Bioenergy Crops. London, UK and Washington DC, USA, Earthscan, 2010.

[7] P. Basu, Combustion and Gasification in Fluidized Beds. Taylor & Francis Group, 2006.

[8] T. R. Bott, Fouling of Heat Exchangers, No. April. Elsevier Science & Technology Books, 1995.

[9] R. W. Bryers, Fireside slagging, fouling, and high-temperature corrosion of heat-transfer surface due to impurities in steam-raising fuels, Progress in Energy and Combustion Science, Vol. 22, No. 1, 1996, pp. 29–120.

[10] J. Chen, X. Lu, Progress of petroleum coke combusting in circulating fluidized bed boilers-A review and future perspectives, Resources, Conservation and Recycling, Vol. 49, No. 3, 2007, pp. 203–216.

[11] Clyde Bergemann Power Group, Diagnostics, website. Available: (accessed on 29.03.2017): http://www.cbpg.com/en/products-solutions-boiler-efficiency-process-optimisation/diagnosis.

[12] E. Coda Zabetta, V. Barisic, K. Peltola, J. Sarkki, T. Jantti, Advanced technology to co-fire large shares of agricultural residues with biomass in utility CFBs, Fuel Processing Technology, Vol. 105, 2013, pp. 2–10.

[13] C. Dechsiri, Particle transport in fluidised beds: experiments and stochastic models. University of Groningen, 2004.

[14] G. Dunnu, J. Maier, G. Scheffknecht, Ash fusibility and compositional data of solid

recovered fuels, Fuel, Vol. 89, No. 7, 2010, pp. 1534–1540.

[15] A. Eklund, Å. Rodin, Sotningsmetodernas effektivitet och konsekvenser på förbränningsanläggningar för olika typer av bränslen, Värmeforsk Service AB, 2004.

[16] Energy Research Centre of the Netherlands, Phyllis2 - Database for biomass and waste, Web database, 2012, website. Available: (accessed on 18.04.2017): https://www.ecn.nl/phyllis2/.

[17] R. Eteläaho, HYBEX Product Training. 2011.

[18] Eurostat, Key figures on Europe 2016 Edition. European Union, 2016.

[19] Eurostat, Municipal Waste Statistics, 2016, website. Available: (accessed on 18.01.2017): http://ec.europa.eu/eurostat/statistics-explained/index.php/Municipal_waste_statistics.

[20] Eurostat, Waste statistics, 2016, website. Available: (accessed on 18.01.2017): http://ec.europa.eu/eurostat/statistics-explained/index.php/Waste_statistics.

[21] R. M. Flores, Coal and Coalbed Gas: Fueling the Future. Elsevier Science, 2013.

[22] F. J. Frandsen, Ash Formation, Deposition and Corrosion When Utilising Straw for Heat and Power Production, Technical University of Denmark, 2011.

[23] B. Gabrielle, H. Wernsdofer, N. Marron, C. Deleuze, Biomass feedstocks, Biomass Supply Chains for Bioenergy and Biorefining, Elsevier, 2016.

[24] M. U. Garba, D. B. Ingham, L. Ma, M. U. Degereji, M. Pourkashanian, A. Williams, Modelling of deposit formation and sintering for the co-combustion of coal with biomass, Fuel, Vol. 113, 2013, pp. 863–872.

[25] A. Garcia-Maraver, J. Mata-Sanchez, M. Carpio, J. A. Perez-Jimenez, Critical review of predictive coefficients for biomass ash deposition tendency, Journal of the Energy Institute, 2016.

[26] GEA, Global Energy Assessment - Toward a Sustainable Future. Cambridge University Press, Cambridge, UK and New York, NY, USA and the International Institute for Applied Systems Analysis, Laxenburg, Austria, International Institute for Applied Systems Analysis, 2012.

[27] D. Geldart, Types of gas fluidization, Powder Technology, Vol. 7, No. 5, 1973, pp. 285–292.

[28] P. Grammelis, Solid Biofuels for Energy. Springer-Verlag London Limited, 2011.

[29] F. Graube, S. Grahl, S. Rostkowski, M. Beckmann, Optimisation of water-cannon cleaning for deposit removal on water walls inside waste incinerators, Waste Management & Research, Vol. 34, No. 2, 2016, pp. 139–147.

[30] T. Hämäläinen, Älykäs nuohous, Promaint, No. 5, pp. 60–61, 2012.

[31] J. Hiljanen, Internal source, Valmet Technologies. 2017.

[32] M. Hupa, Interaction of fuels in co-firing in FBC, Fuel, Vol. 84, No. 10, 2005, pp. 1312–1319.

[33] IEA, World Energy Outlook 2014. International Energy Agency, 2014.

[34] F. Johnsson, The 12th International Conference on Fluidization - New Horizons in Fluidization Engineering Fluidized Bed Combustion for Clean Energy, 12th International conference on Fluidization, 2007.

[35] S. K. Kær, L. A. Rosendahl, L. L. Baxter, Towards a CFD-based mechanistic deposit formation model for straw-fired boilers, Fuel, Vol. 85, No. 5–6, 2006, pp. 833–848.

[36] T. Luomaharju, CYMIC Product Training. Valmet Technologies, 2011.

[37] J. Maier, A. Gerhardt, G. Dunnu, Experiences on Co-firing Solid Recovered Fuels in the Coal Power Sector, Solid Biofuels for Energy, Springer-Verlag London Limited, 2011, p. 247.

[38] I. Mann, K. Boman, A. Stålenheim, L. Nylén, Slagging and fouling – Idbäcken P3 soot blowing evaluation and heat transfer model description, Vattenfall Research and Development AB, 2014.

[39] T. R. Miles, T. R. Miles, L. L. Baxter, R. W. Bryers, B. M. Jenkins, L. L. Oden, Boiler deposits from firing biomass fuels, Biomass and Bioenergy, Vol. 10, No. 2–3, 1996, pp. 125–138.

[40] A. F. Mills, Basic Heat & Mass Transfer, 2nd Editio. Los Angeles, CA, USA, Prentice Hall, Inc., 1999.

[41] F. Moradian, A. Pettersson, T. Richards, Thermodynamic equilibrium model applied to predict the fouling tendency in a commercial fluidized-bed boiler, combusting solid waste, Energy and Fuels, Vol. 29, No. 5, 2015, pp. 3483–3494.

[42] C. Mueller, B.-J. Skrifvars, R. Backman, M. Hupa, Ash deposition prediction in biomass fired fluidized bed boilers - combination of CFD and advanced fuel analysis, Progress in Computational Fluid Dynamics, Vol. 3, No. 2–4, 2003.

[43] H. Namkung, L. Xu, K. Lin, G. Yu, H. Kim, Relationship between chemical components and coal ash deposition through the DTF experiments using real-time weight measurement system, Fuel Processing Technology, Vol. 158, 2017, pp. 206–217.

[44] D. Nutalapati, R. Gupta, B. Moghtaderi, T. F. Wall, Assessing slagging and fouling during biomass combustion: A thermodynamic approach allowing for alkali/ash reactions, Fuel Processing Technology, Vol. 88, No. 11–12, 2007, pp. 1044–1052.

[45] H. Oh, K. Annamalai, J. M. Sweeten, Effects of ash fouling on heat transfer during combustion of cattle biomass in a small-scale boiler burner facility under unsteady transition conditions, International Journal of Energy Research, Vol. 35, 2011, pp.

1236–1249.

[46] S. N. Oka, Fluidized Bed Combustion. Marcel Dekker, Inc., 2004.

[47] B. Peña, E. Teruel, L. I. Díez, Towards soot-blowing optimization in superheaters, Applied Thermal Engineering, Vol. 61, No. 2, 2013, pp. 737–746.

[48] P. Piotrowska, Combustion properties of Biomass Residues Rich in Phosphorus, Åbo Akademi, 2002.

[49] M. Pronobis, Evaluation of the influence of biomass co-combustion on boiler furnace slagging by means of fusibility correlations, Biomass and Bioenergy, Vol. 28, No. 4, 2005, pp. 375–383.

[50] R. Raiko, J. Saastamoinen, M. Hupa, I. Kurki-Suonio, Poltto ja palaminen, Second. International Flame Research Foundation - Suomen kansallinen osasto, 2002.

[51] T. O. Raji, O. M. Oyewola, T. A. O. Salau, New features for performance enhancement of experimental Model Bubbling Fluidized Bed Combustor, International Journal of Scientific & Engineering Research, Vol. 3, No. 1, 2012, pp. 1–10.

[52] K. Rayaprolu, Boilers. CRC Press, 2012.

[53] C. Shen, L. Wang, S. E. Ford, C. Zhang, X. Wang, A novel fouling measurement system : Part I . design evaluation and description, International Journal of Heat and Mass Transfer, Vol. 110, No. July 2017, 2017, pp. 940–949.

[54] R. E. H. Sims, R. N. Schock, A. Adegbululgbe, J. Fenhann, I. Konstantinaviciute, W. Moomaw, H. B. Nimir, B. Schlamadinger, J. Torres-Martínez, C. Turner, Y. Uchiyama, S. J. V. Vuori, N. Wamukonya, X. Zhang, Energy Supply, Climate Change 2007: Mitigation. Contribution of Working Group III to the Fourth Assessment Report of the Intergovernmental Panel on Climate Change, Cambridge University Press, Cambridge, UK and New York, NY, USA, Cambridge University Press, 2007.

[55] P. Sommersacher, T. Brunner, I. Obernberger, Fuel indexes: A novel method for the evaluation of relevant combustion properties of new biomass fuels, Energy and Fuels, Vol. 26, No. 1, 2012, pp. 380–390.

[56] H. Spliethoff, Power Generation from Solid Fuels. Springer-Verlag Berlin Heidelberg, 2010.

[57] A. F. Stam, K. Haasnoot, G. Brem, Superheater fouling in a BFB boiler firing wood-based fuel blends, Fuel, Vol. 135, 2014, pp. 322–331.

[58] T. J. Taha, A. F. Stam, K. Stam, G. Brem, CFD modeling of ash deposition for co-combustion of MBM with coal in a tangentially fired utility boiler, Fuel Processing Technology, Vol. 114, 2013, pp. 126–134.

[59] P. Teixeira, H. Lopes, I. Gulyurtlu, N. Lapa, P. Abelha, Evaluation of slagging and fouling tendency during biomass co-firing with coal in a fluidized bed, Biomass

and Bioenergy, Vol. 39, 2012, pp. 192–203.

[60] M. Theis, Interaction of Biomass Fly Ashes with Different Fouling Tendencies, Åbo Akademi, 2006.

[61] M. Theis, B. J. Skrifvars, M. Zevenhoven, M. Hupa, H. Tran, Fouling tendency of ash resulting from burning mixtures of biofuels. Part 3. Influence of probe surface temperature, Fuel, Vol. 85, No. 14–15, 2006, pp. 2002–2011.

[62] Valmet Technologies, Valmet MyAcademy - CFB Boiler (internal website). .

[63] VDI, VDI Heat Atlas, 2nd ed. Springer-Verlag Berlin Heidelberg, 2010.

[64] R. Weber, M. Mancini, N. Schaffel-Mancini, T. Kupka, On predicting the ash behaviour using Computational Fluid Dynamics, Fuel Processing Technology, Vol. 105, 2013, pp. 113–128.

[65] E. B. Woodruff, H. B. Lammers, T. F. Lammers, Superheaters, Steam Plant Operation, 10th Edition, McGraw Hill Professional, Access Engineering, 2017.

[66] X. Yang, D. Ingham, L. Ma, A. Williams, M. Pourkashanian, Predicting ash deposition behaviour for co-combustion of palm kernel with coal based on CFD modelling of particle impaction and sticking, Fuel, Vol. 165, 2016, pp. 41–49.

[67] A. Zbogar, F. Frandsen, P. A. Jensen, P. Glarborg, Shedding of ash deposits, Progress in Energy and Combustion Science, Vol. 35, No. 1, 2009, pp. 31–56.

[68] M. Zevenhoven-Onderwater, Ash-Forming Matter in Biomass Fuels, Åbo Akademi, 2001.

[69] H. Zhou, P. A. Jensen, F. J. Frandsen, Dynamic mechanistic model of superheater deposit growth and shedding in a biomass fired grate boiler, Fuel, Vol. 86, No. 10–11, 2007, pp. 1519–1533.

[70] S. S. Zumdahl, D. J. DeCoste, Chemical Principles, 7th ed. Brooks/Cole, Cengage Learning, 2013.